



1 Reconstruction of Holocene oceanographic conditions in the
2 Northeastern Baffin Bay

3 *Katrine Elnegaard Hansen¹, Jacques Giraudeau², Lukas Wacker³, Christof Pearce¹, Marit-Solveig*
4 *Seidenkrantz¹*

5 ¹Department of Geoscience, Arctic Research Centre and iClimate, Aarhus University

6 ²Université de Bordeaux, CNRS

7 ³ETH, Zürich

8

9 *Correspondence to:* Katrine Elnegaard Hansen (katrine.elnegaard@geo.au.dk)

10

11 **Abstract**

12 The Baffin Bay is a semi-enclosed basin connecting the Arctic Ocean and the western North
13 Atlantic, thus making out a significant pathway for heat exchange. Here we reconstruct the
14 alternating advection of relatively warmer and saline Atlantic waters versus the incursion of colder
15 Arctic water masses entering the Baffin Bay through the multiple gateways in the Canadian Arctic
16 Archipelago and the Nares Strait during the Holocene. We carried out benthic foraminiferal
17 assemblage analyses, X-Ray Fluorescence scanning and radiocarbon dating of a 738 cm long
18 marine sediment core retrieved from the eastern Baffin Bay near Upernavik (Core AMD14-204C;
19 987 m water depth). Results reveal that the eastern Baffin Bay was subjected to several
20 oceanographic changes during the last 9.2 ka BP. Waning deglacial conditions with enhanced
21 meltwater influxes and an extensive sea-ice cover prevailed in the eastern Baffin Bay from 9.2-7.9
22 ka BP. A transition towards bottom water ameliorations are recorded at 7.9 ka BP by increased
23 advection of Atlantic water masses, encompassing the Holocene Thermal Maximum. A cold
24 period with growing sea-ice cover at 6.7 ka BP interrupts the overall warm subsurface water
25 conditions, promoted by a weaker northward flow of Atlantic waters. The onset of the
26 Neoglaciation at ca. 2.9 ka BP, is marked by an abrupt transition towards a benthic fauna
27 dominated by agglutinated species likely partly explained by a reduction of the influx of Atlantic
28 water, allowing increased influx of the cold, corrosive Baffin Bay Deep Water originating from
29 the Arctic Ocean, to enter the Baffin Bay through the Nares Strait. These cold subsurface water
30 conditions persisted throughout the late Holocene, only interrupted by short-lived warmings
31 superimposed on this cooling trend.

32

33

34



35 **1 Introduction**

36 The opening of the Nares Strait and the narrower gateways of the Canadian Arctic Archipelago
37 (CAA) was initiated towards the end of the last glacial. It was completed in the Early Holocene at
38 9.3-8.3 ka BP, when parts of the Greenland and Innuitian ice sheets, blocking these gateways, had
39 fully retreated from the area (Jennings et al., 2019; Georgiadis et al., 2018; Jennings et al., 2011;
40 England et al., 2006; Zreda et al., 1999). The opening of these gateways presumably had a
41 significant impact on the general oceanic circulation in Baffin Bay and the Labrador Sea, allowing
42 the input of cold Arctic water masses to these regions (Jennings et al., 2019; Jennings et al., 2017).

43 The modern marine environment of Baffin Bay is characterised by a combination of warm Atlantic
44 and cold polar waters. The West Greenland Current (WGC), which flows northward along the
45 coast of West Greenland, carries mixed warm Atlantic-sourced Irminger Current Water and cold
46 and fresh waters of the East Greenland Current (Drinkwater, 1996). The WGC is therefore a major
47 source of Atlantic waters to Baffin Bay, transporting warm and saline water masses to high
48 latitudes. The onset of the present configuration of the WGC during the late glacial (Jennings et
49 al., 2017; Jennings et al., 2018) enabled the advection of Atlantic-sourced waters from the south
50 along the west coast of Greenland into Baffin Bay. These waters progressively expanded from the
51 shelf edge to shallow shelf areas during the deglaciation following the retreat of the Greenland ice-
52 sheet (Jennings et al., 2017; Sheldon et al., 2016). Today, Atlantic water reaches the locations of
53 Thule (76°N) and the southern part of the Nares Strait at its northernmost extension off West
54 Greenland (Buch, 1994; Funder, 1990; Knudsen et al., 2008).

55 Water masses originating from the Arctic Ocean flow southward in the western part of the Baffin
56 Bay (Baffin Current, Fig. 1A), where they act as a substantial contributor of freshwater to the
57 Labrador Sea (Aksenov et al., 2010; Bunker, 1976; Yang et al., 2016). This influence of both cold
58 Polar and warm Atlantic water masses makes Baffin Bay an important area of water mass
59 exchange. Fluctuations in the entrainment of these fresh Polar water masses into the Labrador Sea
60 have been suggested to influence the deep-water formation in the Labrador Sea and thus the
61 Atlantic Meridional Overturning Circulation (AMOC) (Jones and Anderson, 2008; Sicre et al.,
62 2014); consequently, they act as a key element in global heat transport. An increased entrainment
63 of Irminger Current water masses into the WGC leads to local increased air temperatures and
64 contributes to the retreat of marine outlet glaciers of West Greenland facilitated by submarine and
65 surface melting, causing local freshening (Andresen et al., 2011; Jennings et al., 2017).



66 Furthermore, ocean and atmospheric forced melting can contribute to a speed up of the marine
67 outlet glaciers and general instability of the ice dynamics (Holland et al, 2008; Rignot et al, 2010;
68 Straneo & Heimbach, 2013; Straneo et al., 2013).

69 Several studies suggest that the eastern Baffin Bay has been subjected to a series of oceanographic
70 and paleoclimatic changes during the Holocene, induced by changes in the strength of the WGC
71 linked to fluctuations in Atlantic water entrainment and thus to changes in the AMOC. Most of
72 these studies focused on the southern and central shelf regions of West Greenland (Erbs-Hansen
73 et al., 2013; Moros et al., 2015; Lloyd et al., 2007; Perner et al., 2013; Seidenkrantz et al., 2007),
74 but fewer investigated the past dynamics of the WGC in the northeastern sector of Baffin Bay.

75 In this study, we investigate potential changes in the influx of Atlantic-sourced water to the eastern
76 Baffin Bay through the Holocene, discussing the hypothesis that changes in Baffin Bay
77 environmental conditions are closely linked to overall changes in the Atlantic Meridional
78 Overturning Circulation (AMOC). Our study is based on micropalaeontological and geochemical
79 investigations of a marine sediment core retrieved near Upernavik in the Eastern Baffin Bay. This
80 site is located in the flow path of the WGC and in the vicinity of the marine outlet glacier Upernavik
81 Isstrøm (Fig. 1B). Faunal assemblage analysis of benthic foraminifera, radiocarbon datings and X-
82 ray Fluorescence (XRF) data enable the reconstruction of the palaeoceanography and paleoclimate
83 of the northeastern Baffin Bay, including the temporal and spatial development of the water
84 exchange in Baffin Bay during the Holocene.

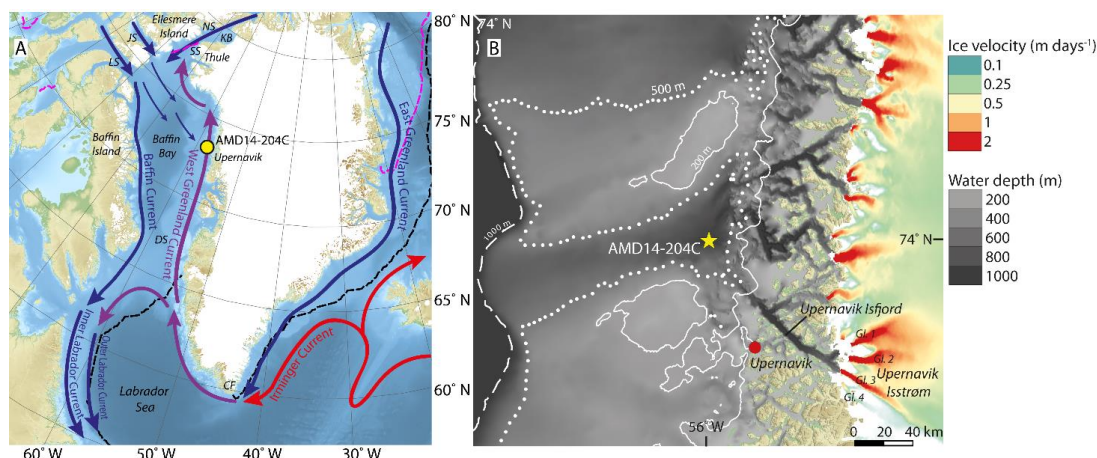
85 **1.1 Regional setting**

86 The Baffin Bay is a semi-enclosed basin constrained by the Baffin Island to the west, Ellesmere
87 Island to the northwest and Greenland to the east (Fig. 1A). The basin is linked to the Atlantic
88 Ocean via the Labrador Sea and the 640 m deep and 320 km wide Davis Strait sill in the south,
89 and is connected to the Arctic Ocean through shallow gateways: Lancaster Sound (125 m deep)
90 and Jones Sound (190 m deep) to the northwest and the deeper Nares Strait (250 m deep) to the
91 north (Tang et al., 2004) (Fig. 1A). The open connections between the Arctic Ocean and Labrador
92 Sea/North Atlantic Ocean makes the Baffin Bay an important area for Polar water export and water
93 mass exchange with the North Atlantic Ocean. The mean water depth in Baffin Bay is <800 m,
94 where the deepest point of the bay in the large central abyssal region exceeds 2300 m water depth
95 (Tang et al., 2004; Welford et al., 2018). An area of maximum 80,000 km² in the northwestern
96 Baffin Bay is occupied by the North Water Polynya (Dunbar & Dunbar, 1972; Tremblay et al.,



97 2002). The prevailing northwesterly winds carry newly formed sea ice away from the polynya,
98 limiting the formation of a thick sea-ice cover resulting in open water conditions, extensive heat
99 loss to the atmosphere and high marine productivity (Melling et al., 2010). The sea ice that is
100 exported from the polynya contributes to brine formation, which may lead to sinking of dense and
101 cold surface waters. The sustainment of the polynya is highly dependent on strong northwesterly
102 winds and the continuous formation of an ice bridge at Smith Sound (Fig. 1A) preventing sea ice
103 from entering Baffin Bay through Nares Strait (Dunbar & Dunbar, 1972; Melling et al., 2010).

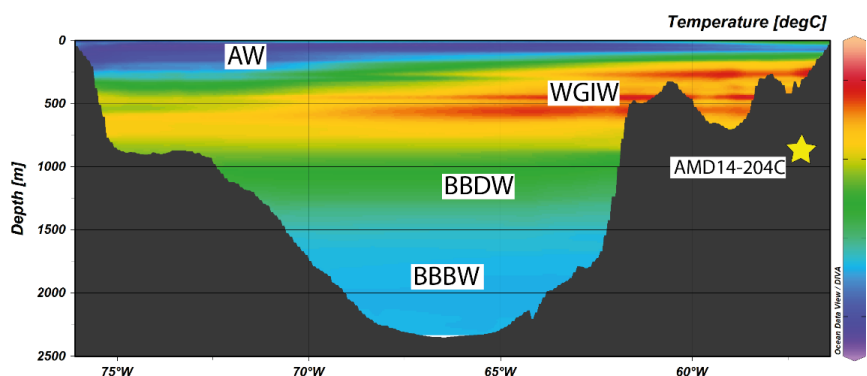
104 The modern ocean surface circulation in Baffin Bay is driven by the local atmospheric circulation
105 system affecting the strength of the northwesterly winds, creating an overall cyclonic ocean
106 circulation pattern (Drinkwater, 1996) (Fig. 1A). From the south near Cape Farewell, the mixed
107 WGC carries relatively warm saline water from the Irminger Current (IC) and cold ice loaded
108 Polar waters from the East Greenland Current (EGC) towards the north over the shelf region of
109 the West Greenland margin (Drinkwater, 1996), creating the West Greenland Intermediate Water
110 (Tang et al., 2004). The IC water component is mainly constrained to the continental slope in the
111 depth range of 200-1000 m, whereas the EGC component is more shelf oriented and thus shallower
112 (200 m), (Buch, 1994; Rykova et al., 2015). The WGC bifurcates into two branches when reaching
113 Davis Strait (Cuny et al., 2002). Here, one branch flows towards the west and eventually meets
114 and joins the Outer Labrador Current and heads south (Cuny et al., 2002; Drinkwater, 1996). The
115 other WGC branch continues northward along the west coast of Greenland and at turns westwards
116 at 75 °N, where it mixes with Arctic waters entering the Baffin Bay from the north through Nares
117 Strait and the gateways in the Canadian Arctic Archipelago (CAA) (Drinkwater, 1996). These
118 combined water masses make up the Baffin Current (BC), which comprises a major part of the
119 freshwater content in the southward flowing Labrador Current (Mertz et al., 1993). Parts of the
120 surface outflow from the CAA gateways recirculate eastward to the northeastern Baffin Bay
121 (Landry et al, 2015). The relative contribution of water masses from the IC and EGC plays a
122 prominent role in the temperature and salinity signature of the WGC.



123

124 **Figure 1** A: Map showing the study site and the modern ocean surface circulation. Red, blue and purple arrows represents warmer,
 125 colder and mixed/intermediate water temperatures, respectively. The core AMD14-204C is marked with the yellow circle. The
 126 pink and black dashed lines mark the median sea-ice extent from 1981-2010 in September and March respectively (NSIDC, 2019).
 127 Abbreviations: LS = Lancaster Sound, JS = Jones Sound, NS = Nares Strait, SS = Smith Sound, KB = Kane Basin, DS= Davis
 128 Strait, CP = Cape Farewell. B: Close up on the Upernavik Isstrøm area, showing the local bathymetry and ice stream velocities.
 129 The Upernavik Isstrøm is comprised by four glaciers. The ocean bathymetry and bed topography data is derived from GEBCO
 130 (Weatherall et al., 2015) and BedMachine v3(Morlighem et al., 2017) and the ice stream velocity data is derived from Sentinel-1
 131 SAR data acquired from 2017-12-28 to 2018-02-28 (Nagler et al., 2015). Abbreviations: Gl. = glacier.

132 The deeper part of the Baffin Bay (1200-1800 m water depth) is subjected to the cold, saline Baffin
 133 Bay Deep Water (BBDW). Water masses at depths exceeding 1800 m are referred to as Baffin
 134 Bay Bottom Water (BBBW) (Tang et al., 2004) (Fig. 2). Several hypotheses for the source of these
 135 water masses include local brine production in connection with winter sea ice formation on the
 136 shelf (Tan & Strain, 1980), cooled subsurface waters from Kane Basin flowing in via Nares Strait
 137 in a pulse like manner (e.g. Aksu, 1981; Collin, 1965), and the migration of cold, saline waters
 138 produced at the North Water Polynya (Bourke & Paquette, 1991).



139

140 **Figure 2**: Water temperature transect at 73°N showing the different water masses. The yellow star indicate the core site at 987 m
 141 water depth. Abbreviations: AW = Arctic Water (0-300 m), WGIW = West Greenland Intermediate Water (300-800 m), BBDW =



142 Baffin Bay Deep Water (1200-1800 m), BBBW = Baffin Bay Bottom Water (1200-1800 m), (Tang et al., 2004). Temperature data
143 from World Ocean Atlas (Locarnini et al., 2013).

144 The modern sea-ice duration in Baffin Bay is longest in its north-western sector, and shortest in its
145 eastern region influenced by the northward flow of the warmer WGC (Tang et al., 2004; Wang et
146 al., 1994). Sea ice starts forming in open waters in the north and most of the bay is fully covered
147 by sea ice by March. In September, sea ice is limited to the CAA, and Baffin Bay is primarily
148 influenced by a sporadic thinner sea-ice cover (Tang et al., 2004) (Fig. 1A).

149 The shelf region of West Greenland is incised by numerous canyons and fjords among which
150 Upernavik Isfjord is the nearest to our core site (Fig. 1B). The fast-flowing marine-based outlet
151 glaciers that make up Upernavik Isstrøm terminate in the Upernavik Isfjord (Fig. 1B) (Briner et
152 al., 2013). Results from previous studies suggest that retreats of the ice stream are influenced by
153 the advection of warmer Atlantic waters into the fjord (Andresen et al., 2014; Vermassen et al.,
154 2019).

155 **2 Material and methods**

156 The presented multiproxy study is based on the analysis of marine sediment core AMD14-204C,
157 a Calypso Square (CASQ) gravity core collected on board the Arctic research vessel, Canadian
158 Coast Guard Ship (CCGS) *Amundsen* as part of the ArcticNet leg 1b expedition in 2014. The 738
159 cm long core was retrieved from 987 m water depth, in northeastern Baffin Bay (73°15.663'
160 N/57°53.987' W) at the head of the Upernavik Trough near Upernavik Isstrøm (Fig. 1). Shortly
161 after retrieval, the 738 cm long gravity core was subsampled into five core sections on board the
162 research vessel using 150 cm-long U-channels. These were subsequently kept in cold storage.

163

164 **2.1 Chronology**

165 The age model for core AMD14-204 C is based on 11 AMS (Accelerator Mass Spectrometry)
166 radiocarbon dates, mainly consisting of mixed benthic foraminiferal species. One sample also
167 contains some mixed ostracod species and two samples encompass both benthic and planktonic
168 foraminifera due to the scarcity of calcareous material in the core, see Table 1. Four of these mixed-
169 species radiocarbon dates have previously been used in an earlier version of the age model (Caron
170 et al., 2018;), and our revised age model includes seven additional levels of radiocarbon dates
171 measured at the ETH Laboratory, Ion Beam Physics in Zürich, see Table 1 and Supplementary for
172 further details on the method. These latter samples are based on either pure benthic or pure
173 planktonic species; for four of the levels we could date both samples based on benthic and on



174 planktonic specimens, where only the samples with benthic species were used in the age model.
 175 All conventional radiocarbon ages were calibrated using the Marine13 radiocarbon calibration data
 176 (Reimer et al., 2013) with the OxCal v4.3 software (Ramsey, 2008). A marine reservoir correction
 177 of $\Delta R = 140 \pm 30$ years has previously been used in similar studies of the Baffin Bay and west
 178 Greenland area (e.g. Lloyd et al., 2011, Perner et al., 2012, Jackson et al., 2017) and is therefore
 179 used in the calibration of the radiocarbon dates in this study.

180 **Table 1:** List of radiocarbon dates and modelled ages in core AMD14-204C. The dates with a * sign have previously been published
 181 in Caron et al., 2018. All dates were calibrated using the Marine13 calibration curve (Reimer et al 2013) and $\Delta R = 140 \pm 30$ years.

Sample depth midpoint (cm)	Lab. ID	Material	^{14}C age (yr BP)	Calibrated age range (cal yr. BP), 1σ	Modelled median age (cal. yr BP)
4.5	ETH-92277	Mixed benthic foraminifera	705 \pm 50	167-276	213
70.5	ETH-92279	Mixed benthic foraminifera	1795 \pm 50	1175-1270	1216
70.5	ETH-92278	Mixed planktonic foraminifera	1710 \pm 50	1032-1175	1101
170*	SacA 46004	Mixed benthic & planktonic foraminifera	3555 \pm 35	3139-3260	3192
250.5*	BETA 467785	Mixed benthic & planktonic foraminifera	4300 \pm 30	4133-4254	4199
310.5	ETH-92281	Mixed benthic foraminifera	4950 \pm 60	4860-4992	4941
310.5	ETH-92280	Mixed planktonic foraminifera	4940 \pm 70	4930-5188	5043
410.5	ETH-92283	Mixed benthic foraminifera	5805 \pm 60	5905-6005	5959
410.5	ETH-92282	Mixed planktonic foraminifera	5825 \pm 60	5984-6155	6063
501.5*	BETA 488641	Mixed benthic foraminifera	6400 \pm 30	6656-6751	6707
580.5	ETH-92285	Mixed benthic foraminifera	7155 \pm 70	7430-7531	7483
580.5	ETH-92284	Mixed planktonic foraminifera	7005 \pm 60	7298-7417	7356
610*	SacA 46005	Mixed benthic foraminifera & ostracods	7445 \pm 50	7712-7822	7766
700.5	ETH-92286	Mixed benthic foraminifera	8270 \pm 389	8639-8885	8755
737.5	ETH-92287	Mixed benthic foraminifera	8489 \pm 154	9017-9302	9162

182

183 2.2 Foraminifera

184 Sediment samples of 1 cm width were subsampled every 10 cm throughout most of the core for
 185 foraminiferal analyses, except for the 500-503 cm interval, the top (4-5cm) and bottom (737-738
 186 cm) of the core where every 1 cm was counted and subsequently used for radiocarbon dating. The



187 wet sediment samples were weighed followed by wet sieving using sieves with mesh sizes of
188 0.063, 0.100 and 1 mm. Each fraction was dried in filter paper in the oven at 40 °C overnight
189 before they were weighed and stored in glass vials. For the benthic foraminiferal assemblage
190 analyses, the 0.063 and 0.100 mm fractions were combined, and both calcareous and agglutinated
191 species were identified and counted together in order to reach sufficient total counts for reliable
192 assemblage analyses. In all cases we were able to identify at least 300 benthic individuals,
193 following the method used in (Lloyd et al., 2011; Perner et al., 2011; Perner et al., 2012).

194

195 **2.3 X-ray Fluorescence**

196 The non-destructive X-ray Fluorescence (XRF) method allows the measurement of changes in the
197 bulk geochemical elemental compositions of the core without disturbing the sediment. The core
198 was scanned and logged in 5 mm steps using an AVAATECH scanner at the EPOC laboratory in
199 Bordeaux. The scan was conducted with generator settings of 10, 30 and 50 kV using a Rhodium
200 (Rh) tube in order to get the full elemental spectra from Al to Ba. Data have previously been
201 presented by Giraudeau et al., (submitted).

202

203 **3 Results**

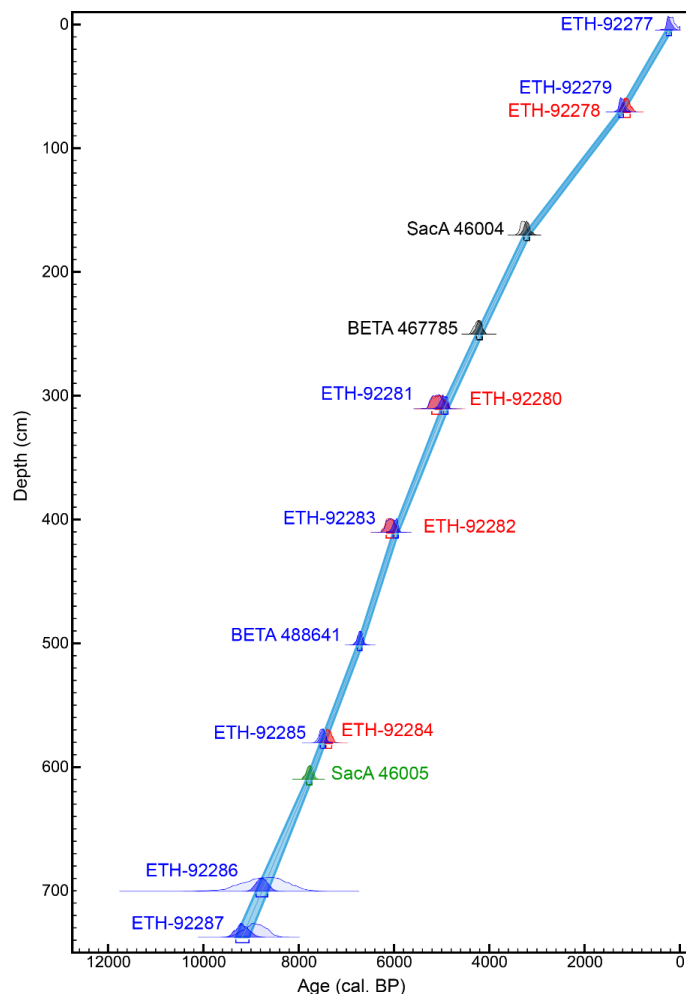
204 **3.1 Core description**

205 The core primarily consists of hemipelagic mud. The lowermost part of the core (738-610 cm) is
206 composed of greyish brown (2.5 Y/4/2) homogenous clayey silt, transitioning to bioturbated, olive
207 grey (5Y 4/2) clayey silt in the upper part of the core (Caron et al., 2018).

208

209 **3.2 Chronology**

210 In previous studies of Core AMD14-204C (Caron et al., 2018; Giraudeau et al., submitted) age
211 models were based on radiocarbon dating of bulk sediment samples, and paleomagnetic markers,
212 with only a few foraminifera ¹⁴C dates. Our present study includes several new radiocarbon dates
213 on foraminifera, and therefore no longer includes the bulk datings. Our 11 calibrated ¹⁴C dates,
214 primarily based on foraminifera, reveal that the 738 cm-long sediment core encompasses the last
215 ca. 9200 cal. years BP, covering most of the Holocene (Fig. 3). For the age depth modelling, a
216 depositional P_sequence model was used with a k-value of 0.68 (Ramsey, 2008). The average
217 sedimentation rate for the core is 86 cm/k year.



218

219 **Figure 3:** Age model for core AMD14-204C based on 11 radiocarbon dates (the green, black and blue dates). The light blue
220 envelope represents the modelled 1σ range, and the blue line marks the modelled median age. The light shaded areas for each
221 radiocarbon date indicate the probability distribution prior age modelling whereas the darker areas indicate the posterior probability
222 distribution. Blue; mixed benthic foraminifera, red; mixed planktonic foraminifera, grey; mixed planktonic and benthic
223 foraminifera, green; mixed ostracods, planktonic and benthic foraminifera.

224 Pairs of mixed benthic and mixed planktonic calibrated ^{14}C dates measured at the same sample
225 depths 70.5, 310.5, 410.5 and 580.5 show only small differences (Fig. 3), all of which lie within
226 the same age uncertainty. These results suggest that the radiocarbon ages measured from samples
227 of mixed benthic and planktonic species are reliable. Today, the water carried by the WGC
228 occupies the whole water column over the continental margin of eastern Baffin Bay (Cuny et al.,
229 2002; Tang et al., 2004). The similar dates obtained from pairs of planktonic and benthic
230 foraminifera specimens in samples from the top to the bottom part of the core suggest that, at our

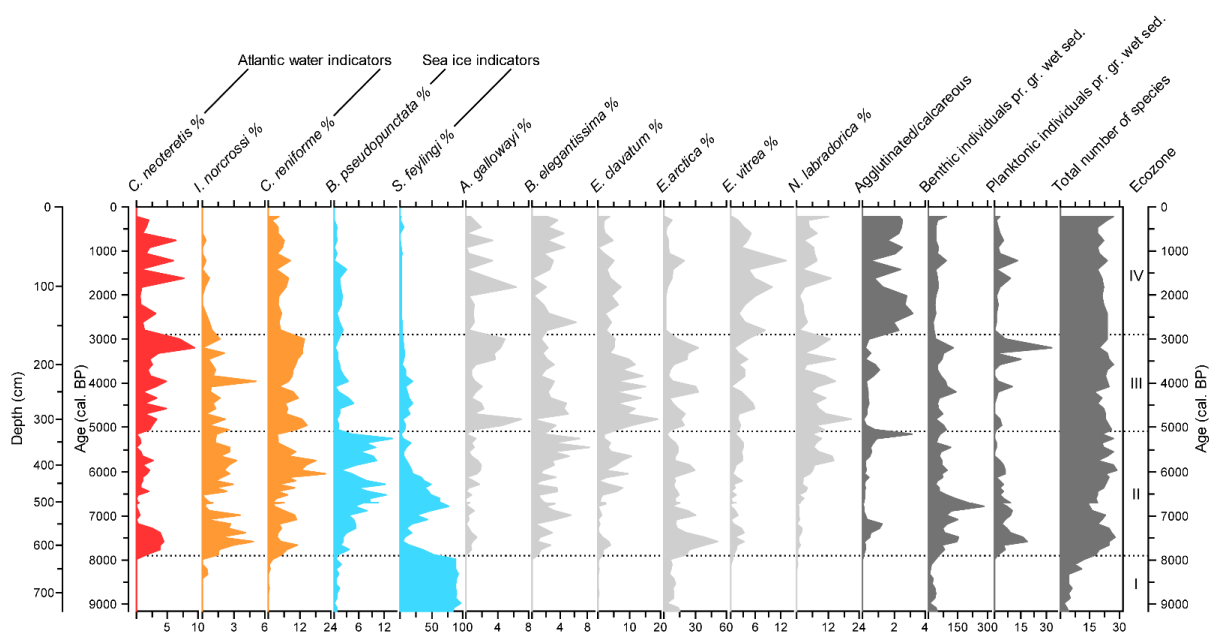


231 study site, the subsurface and bottom waters were subjected to the same water mass throughout
232 the Holocene.

233

234 3.3 Foraminifera

235 The agglutinated and calcareous benthic foraminiferal tests were in general well preserved
236 throughout the core and there were minor signs or no signs of post mortem dissolution of the tests.
237 A total of 43 calcareous and 17 agglutinated benthic foraminiferal taxa were identified. The
238 relative abundances in percent were calculated from the entire benthic foraminiferal assemblages
239 (combined agglutinated and calcareous foraminiferal specimens assemblage to allow statistically
240 sufficient count numbers), and the benthic species shown in the figures all have a percentage
241 frequency of 4 % in at least one of the sample intervals of the core (Fig. 4 and 5). Planktonic
242 foraminiferal specimens are on average 10 times less abundant than benthic specimens, with the
243 lowest abundance at the bottom of the core. A down core succession of four ecozones was defined
244 based on major changes in the relative abundance of the most abundant benthic species, indicative
245 of changes in the environment.

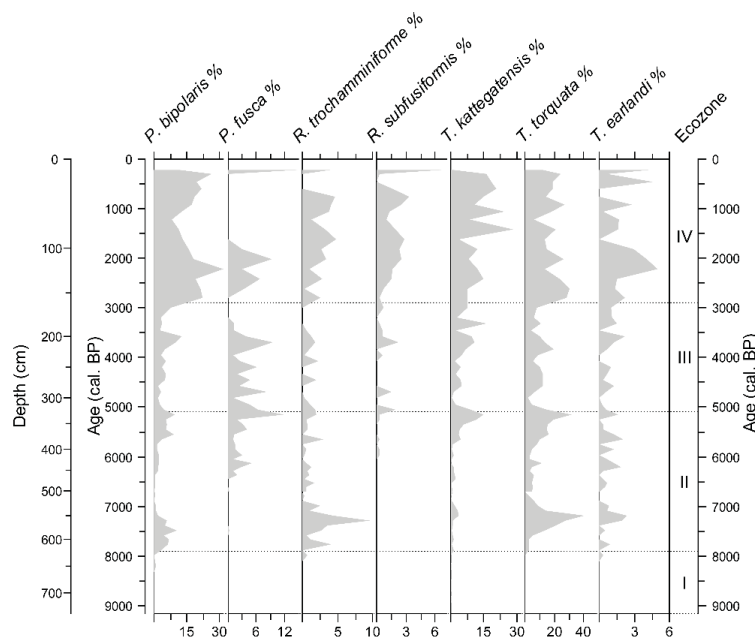


246

247 **Figure 4:** Downcore distribution of the most abundant (>4% in at least one sample) calcareous benthic foraminiferal species.
248 Ecozones (I to IV) are shown on the right side of the figure. Relative abundances are calculated based on the entire benthic
249 (calcareous and agglutinated) foraminiferal assemblage. Some species are grouped (colour shading) according to their known
250 environmental preferences (see references in text): red: warm Atlantic water; orange: chilled Atlantic water; light blue: sea ice.



251



252

253 **Figure 5:** Down core distribution of the most abundant (>4% in at least one sample) agglutinated benthic foraminiferal species.
254 Ecozones (I to IV) are given on the right side of the figure. Relative abundances are calculated based on the entire benthic
255 (calcareous and agglutinated) foraminiferal assemblage.

256 ***Ecozone I: 9.2-7.9 cal. ka BP:***

257 This ecozone is highly dominated by the species *Stainforthia feylingi*, which contributes to almost
258 100 % of the benthic foraminiferal fauna. Only a few other species are represented here with
259 abundances so low that they are considered insignificant. The foraminiferal concentrations are the
260 lowest of the entire record, and planktonic specimens as well as agglutinated benthics are absent.

261 ***Ecozone II: 7.9-5.1 cal. ka BP***

262 The base of this ecozone is defined by a sudden increase in benthic species diversity and in both
263 benthic and planktonic foraminiferal abundances. The abundance of *S. feylingi* decreases. Instead,
264 *Cassidulina neoteretis*, *Cassidulina reniforme*, and *Islandiella norcrossi* show high abundances
265 centred around 7.4 ka BP and again at 6 ka BP, separated by a very low abundance at 6.7 ka BP,
266 coinciding with a general low species diversity and a temporary increase in *S. feylingi* and the
267 common occurrence of *Bolivinelina pseudopunctata*. These two latter species combined
268 constitute 70 % of the fauna at 6.7 ka BP. Overall the abundances of the two species groups made
269 of *S. feylingi* – *B. pseudopunctata*, on one hand, and *C. neoteretis* – *C. reniforme* – *I. norcrossi*, on
270 the other hand seem to be anti-correlated. Also noticeably is the significant abundance of up to 50



271 % of *Epistominella arctica* in the beginning of the ecozone. Characteristic for the end of the
272 ecozone is the large relative abundance of the agglutinated species compared to the calcareous
273 benthic fauna, again coinciding with a peak abundance of *B. pseudopunctata* and a drop in
274 frequencies of *C. neoteretis*, *C. reniforme*, and *I. norcrossi*. The most abundant agglutinated
275 species are *Portatrochammina bipolaris*, *Recurvoides trochamminiforme* and *Textularia torquata*.

276 ***Ecozone III: 5.1-2.9 cal. ka BP***

277 Overall, this ecozone is characterized by fluctuating abundances of many species. Both *Elphidium*
278 *clavatum* and *Nonionellina labradorica* show higher but fluctuating abundances compared to the
279 previous ecozone. The frequency of *E. arctica* peaks three times in this ecozone, reaching
280 abundances of around 30 %. Both *B. pseudopunctata* and *S. feylingi* display low abundances of
281 <1-5 % and 3-20 % respectively, while the decrease of *B. pseudopunctata* is very sudden in the
282 beginning of the ecozone. *C. neoteretis*, *C. reniforme* and *I. norcrossi* show a combined abundance
283 of 8-23 %. The relative frequencies of *Astrononion gallowayi* and *Buliminella elegantissima* tend
284 to be anti-correlated, with peak abundances of *A. gallowayi* in the beginning (7 %) and end (5 %)
285 of the ecozone corresponding to low (0 and 1 %, respectively) contributions of *B. elegantissima*.
286 The highest abundances of planktonic foraminifera for the entire core occurs in this ecozone at 3.2
287 ka BP. The abundance of agglutinated species is in general low but the frequency of
288 *Psammosphaera fusca* is relatively high, together with *Textularia kattegatensis* and *T. torquata*.

289 ***Ecozone IV: 2.9-0.2 cal. ka BP***

290 This ecozone is characterized by a sudden increase of the agglutinated/calcareous benthic species
291 ratio, as the agglutinated specimens outnumber the benthic calcareous individuals by a factor of
292 three. *P. bipolaris*, *T. kattegatensis* and *T. torquata* are among the most abundant agglutinated
293 species in this ecozone. The dominance of agglutinated species coincides with a drop in the
294 contributions of planktonic foraminifera as well as of the benthic species *C. neoteretis*, *C.*
295 *reniforme* and *I. norcrossi*. The high abundances of agglutinated species persist towards the top of
296 the core, only interrupted by three periods of lower values at 1.6 ka BP, 1.2 ka BP and 0.8 ka BP,
297 corresponding to intervals with high contribution of *C. neoteretis* (6-8 %) and *C. reniforme* (6-8
298 %). *I. norcrossi* is in general poorly represented in this ecozone (< 1 %), while the percentage
299 frequency of *C. reniforme* is generally stable but lower than in ecozone II and III. *Epistominella*
300 *vitrea* experiences its highest mean relative abundance of the entire core within ecozone IV,
301 peaking at 1.2 ka BP (13 %). *E. clavatum*, *E. arctica* and *N. labradorica* abundances decrease



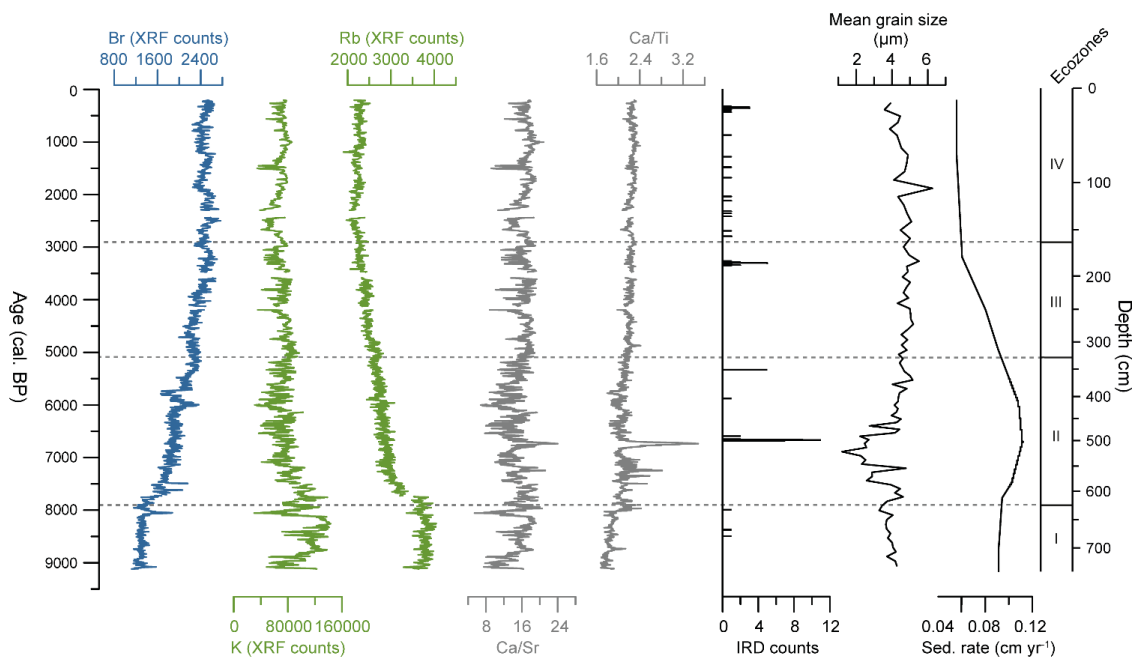
302 compared to the preceding ecozone and both *S. feylingi* and *B. pseudopunctata* are poorly
303 represented in this ecozone

304

305 **3.4 Geochemistry**

306 The XRF record shows several smaller events in addition to a general down-core pattern (Fig. 6).
307 Giraudeau et al. (submitted) interpreted the elemental composition of this core in relation to
308 provenance of source sediments. Here we primarily focus on the terrestrial vs. marine signal.
309 Ecozone I is characterized by relatively low values of Br and Ca/Ti while the K and Rb counts are
310 high. Br counts increase throughout Ecozone II-III and become more or less stable in Ecozone IV.
311 The opposite pattern characterize the K and Rb counts. Both the Ca/Sr and Ca/Ti ratios are
312 relatively stable throughout the core; though, a slight increasing trend is seen in the Ca/Ti ratio
313 towards Ecozone IV. Both ratios show a prominent peak at around 6.7 ka BP in Ecozone II
314 coinciding with the highest values of IRD concentrations in the core.

315 We consider the element Br as an indicator of marine biological productivity often associated with
316 high amounts of marine organic matter (Pruysers et al., 1991). High counts of this element
317 therefore indicate minimal contribution of terrestrial-sourced material to the bulk sediment
318 (Calvert and Pedersen, 1993; Rothwell and Croudace, 2015). K and Rb are both typical for
319 environments with terrestrial influence (Saito, 1998; Steenfelt, 2001; Steenfelt et al., 1998). The
320 Ca/Ti and Ca/Sr ratios can be used as indicators of the marine biogenic origin of Ca (Bahr et al.,
321 2005; Richter et al., 2005). IRD counts and the mean grain size record are both indicators of
322 terrestrial influence, since larger grain sizes can be related to iceberg calving and or increased
323 sediment delivery by the Upernavik Isstrøm. More information about these two records is available
324 in Caron et al. (2018) and Giraudeau et al (submitted).



325

326 **Figure 6: From left to right:** X-ray fluorescence data, IRD concentration, mean grain size expressed in μm (Caron et al., 2018),
327 and sedimentation rate in core AMD14-204C. The benthic foraminiferal ecozones are given in the right-most part of the plot. Gaps
328 in data indicate missing data.

329 4 Paleoenvironmental interpretation

330 The distributional patterns of foraminiferal assemblages are indicators of changes in bottom and
331 subsurface water conditions. Changes in the abundance ratio of agglutinated vs. calcareous
332 specimens in sediments of Baffin Bay are often interpreted as evidence of subsurface deterioration,
333 occasionally linked to the influx of the cold, saline and corrosive CO_2 -rich Baffin Bay Deep Water
334 (BBDW) (Jennings, 1993; Jennings & Helgadottir, 1994; Knudsen et al., 2008; Schröder-Adams
335 & Van Rooyen, 2011). Off West Greenland, *I. norcrossi* and *C. neoteretis* are generally considered
336 indicators of increased advection of Atlantic IC water into the WGC, based on their preference of
337 relatively warm and high salinity waters (Knudsen et al., 2008; Perner et al., 2013; Seidenkrantz,
338 1995; Lloyd, 2006), albeit with *I. norcrossi* likely tolerating colder conditions and increased
339 mixing with Polar water compared to *C. neoteretis*. *C. reniforme* has also been used as an indicator
340 species for chilled Atlantic water, since it can live in somewhat colder and more saline water
341 masses than the other Atlantic water indicator species presented here (Ślubowska-Woldengen et
342 al., 2007). High abundances of *S. feylingi* and *B. pseudopunctata* are often considered associated
343 with high primary productivity in the proximity of sea-ice edges; both species are tolerant to
344 reduced bottom-water oxygen content (Knudsen et al., 2008; Seidenkrantz, 2013; Sheldon et al.,



345 2016). According to Seidenkrantz (2013), *S. feylingi* can be regarded as a typical sea-ice edge
346 indicator species. These micropaleontological proxy data, together with geochemical (XRF core
347 scanner-derived) and sedimentological data allow us to infer paleoenvironmental conditions within
348 each periods defined by the four foraminiferal ecozones.

349

350 ***Ecozone I: 9.2-7.9 cal. ka BP:***

351 The total dominance of *S. feylingi* prior to 7.9 ka BP implies that conditions were unfavourable for
352 other foraminiferal species. *S. feylingi* is an opportunistic species, which can tolerate unstable low
353 oxygen conditions at the sea floor related to a stratified water column (Knudsen & Seidenkrantz,
354 1994; Patterson et al., 2000). The relatively high counts of the terrestrially-derived elements K, Rb
355 and a low Ca/Ti ratio, together with relatively high sedimentation rates (0.092 cm/year) could
356 indicate increased meltwater influence from the Greenland Ice Sheet. Furthermore, the low Br
357 counts and low absolute abundance of foraminifera imply that the general marine productivity was
358 low (Calvert and Pedersen, 1993; Pruyers et al., 1991). The absence of Atlantic water indicator
359 species suggests a weakening of the Atlantic water entrainment into the WGC, possibly in
360 connection with a WGC flow path located further away from the shelf. From 9.2 to 7.9 ka BP, the
361 eastern Baffin Bay region was therefore characterized by continuous meltwater injections from the
362 Greenland Ice Sheet (GIS) and an extensive sea-ice cover, associated with the final phase of the
363 deglaciation.

364 ***Ecozone II: 7.9-5.1 cal. ka BP:***

365 The overall increase in species diversity from 7.9 ka BP indicates a transition towards ameliorated
366 subsurface conditions with higher marine biogenic productivity. The general decrease in Rb, K
367 and mean grain size together with increasing Br values point to a smaller influence of terrestrially-
368 derived sediment, possibly related to reduced meltwater inputs from the retreating Greenland Ice
369 Sheet.

370 These improved subsurface conditions were plausibly facilitated by a stronger entrainment of
371 Atlantic water masses into the WGC, inferred from the high contribution to the foraminiferal
372 assemblages of Atlantic water indicator species together with an increase in *P. bipolaris* which has
373 previously been linked to the presence of Atlantic water in the nearby Disko Bugt (Wangner et al.,
374 2018). The Atlantic water incursion seems especially strong at around 7.4 ka BP, coinciding with
375 an increase in planktonic foraminifera, indicative of increasing air temperatures and warming of



376 the (sub)surface waters, and further supported by the low abundances of the benthic sea-ice
377 indicator species. Particularly the low abundance of *S. feylingi* coinciding with high percentages
378 of *E. arctica* point to a reduction of the sea-ice cover, but high productivity (Seidenkrantz, 2013;
379 Wollenburg & Mackensen, 1998).

380 The advection of Atlantic waters decreased significantly at 6.7 ka BP, as indicated by the sudden
381 decrease in abundances of Atlantic water indicator species and a decrease in planktonic
382 foraminifera. An increase in benthic sea-ice indicator species and an overall low benthic
383 foraminiferal species diversity implies that the area was subjected to colder air temperatures,
384 associated with an expansion of the sea-ice cover and a worsening in the subsurface conditions.
385 Additionally, the transition towards higher abundance of benthic sea-ice species coincides with a
386 large abundance peak of the agglutinated cold-water species *T. torquata* (Perner et al., 2012;
387 Wangner et al., 2018). The peak values in the Ca/Ti Ca/Sr ratio around 6.7 ka BP suggest that a
388 high amount of carbonate was exported to the area, possibly deposited as ice-rafted debris (IRD)
389 according to the synchronous high IRD counts (Fig. 6). Previous studies have described the
390 presence of detrital carbonate in the Baffin Bay, related to deposition by icebergs and or sea ice
391 (e.g. Andrews et al., 2011; Jackson et al., 2017). This short-lived cold period at 6.7 ka BP can be
392 related to a temporarily weaker incursion of Atlantic water off western Greenland, enabling cold
393 Polar waters to enter the Baffin Bay, either in the form of increased EGC entrainment into the
394 WGC and as Polar water delivered from the CAA. The event may potentially designate a very late
395 meltwater event affecting the ocean circulation, but further investigations are needed to test this
396 hypothesis.

397 At ca 6.0 ka BP, the Atlantic water contribution to WGC again increased, while sea ice retreated,
398 based on the high frequency of the Atlantic water indicator species and the low abundance of sea-
399 ice indicator species. The prevailing conditions were similar to those around 7.4 ka BP, but the
400 lower abundances of the true Atlantic water indicator species *C. neoteretis* (cf. Seidenkrantz,
401 1995), implies that subsurface conditions were not as warm as around 7.4 ka BP.

402 The high agglutinated/calcareous foraminiferal ratio coinciding with low abundance of the Atlantic
403 water indicator species just prior to 5.1 ka BP implies a short period of cold and corrosive
404 subsurface waters, unfavourable for most of the calcareous benthic species. However, these
405 conditions were favourable for the opportunistic benthic species *B. pseudopunctata*, which has
406 been linked to environments with low oxygen conditions (Gustafsson and Nordberg, 2001;



407 Patterson et al., 2000). This deterioration of the subsurface environment can possibly be ascribed
408 to a decreasing strength of the WGC together with a presumably reducing Atlantic water
409 entrainment and a stronger influence of the cold corrosive BBDW.

410 ***Ecozone III: 5.1-2.9 cal. ka BP***

411 A general amelioration of the bottom water environment and decreasing sea-ice cover, promoted
412 by a stronger Atlantic water entrainment at 5.1 ka BP, is suggested by an increased contribution
413 of Atlantic-water species and decreasing abundances of *B. pseudopunctata* and *S. feylingi*. High
414 contributions of *A. gallowayi* and *E. clavatum* imply that the hydrodynamic activity at the sea floor
415 was high and unstable in the beginning and end of the ecozone (Knudsen et al., 1996; Korsun &
416 Hald, 2000; Polyak et al., 2002), hereby related to a strengthening of the WGC flow.

417 The low abundances of *B. elegantissima* are possibly caused by the high turbidity levels. High
418 salinities linked to the strong entrainment of Atlantic derived water masses can also be inferred for
419 this time period considering the tolerance of *A. gallowayi* for raised salinity conditions (Korsun &
420 Hald, 1998). This fits well with the synchronous higher contributions of *C. reniforme*, which
421 previously has been associated with the incursion of chilled saline Atlantic waters (Ślubowska-
422 Woldengen et al., 2007).

423 The primary productivity species *N. labradorica* is often associated with the presence of fresh
424 phytodetritus in relation to primary productivity blooms and oceanic fronts (Jennings et al., 2004;
425 Polyak et al., 2002; Rytter, 2005). At our study site, this species seems to thrive under generally
426 warm bottom water conditions. *E. arctica* and *E. vitrea*, which are also both productivity indicators
427 (Perner et al., 2013; Scott et al., 2008; Wollenburg & Kuhnt, 2000; Wollenburg & Mackensen,
428 1998), show somewhat more fluctuating distributions in this ecozone, which could be linked to
429 shifting nutrient supply and fluctuating turbidity at the bottom. The overall high abundances of the
430 benthic productivity indicators reveal improved bottom water conditions with high food
431 availability.

432 ***Ecozone IV: 2.9-0.2 cal. ka BP***

433 The sudden drop in calcareous foraminiferal concentrations illustrated by the very sudden increase
434 in the agglutinated/calcareous benthic ratio suggests that the decrease in the abundance of
435 calcareous specimens is most likely not a result of poor post-mortem preservation of these species
436 within the core, but rather related to environmental changes in the bottom waters. This is also
437 supported by the fact that the calcareous specimens are well preserved after 2.9 ka BP. We suggest



438 that the unfavourable conditions for the calcareous benthic foraminifera are associated with an
439 increasing influx of BBDW, impeding test formation of the calcareous species, because of the cold
440 corrosive property of this deep water mass. The increased inflow of BBDW was presumably
441 promoted by an overall weaker WGC flow and a diminishing entrainment of Atlantic water into
442 the WGC, as inferred from the phased decrease in abundance of Atlantic water indicator species.
443 Additionally, the lower sedimentation rate (0.056 cm/year) throughout this ecozone could possibly
444 be yielded by a weaker WGC flow strength. However, the continued, albeit lower, presence of
445 Atlantic water species and well-preserved calcareous specimens indicates some continued, at least
446 intermittent, influx of Atlantic water.

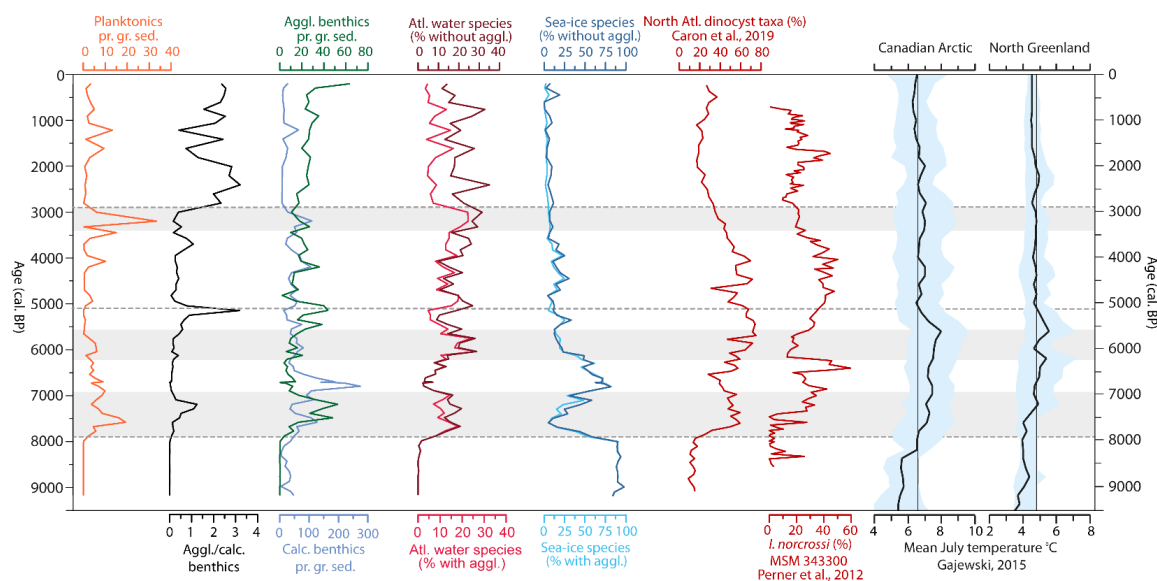
447 The short-term events of increased abundances of Atlantic water indicator species and high
448 planktonic foraminiferal concentrations centred roughly at 1.6, 1.2 and again at 0.8 ka BP are
449 possibly linked to periods of strengthening of the Atlantic water entrainment into the WGC,
450 resulting in short-term amelioration of the bottom and surface water conditions. The re-
451 strengthening of the WGC flow is supported by coinciding peak abundances of *A. gallowayi*
452 (Polyak et al., 2002). The productivity indicator species *E. vitrea* seems to favour conditions with
453 a relatively strong WGC possibly associated with the introduction of certain nutrients to the area.
454 Although the overall colder bottom water conditions could be expected to induce increased sea-
455 ice cover, conditions do not seem to have been favourable for the sea-ice indicator species *S.*
456 *feylingi* and *B. pseudopunctata*. However, these species are particularly thin-shelled and thus
457 highly sensitive to corrosive bottom water conditions.

458 **5 Discussion**

459 The interpretations of the benthic foraminiferal assemblage fauna and XRF data from this study,
460 suggest that several oceanographic and climatic changes, occurred during the Holocene in the
461 eastern Baffin Bay, associated with the relative change of Atlantic water mass advection, influence
462 of ice sheets, inflowing water masses derived from the Arctic Ocean, and the extent of sea-ice
463 cover. The changes herein are summarized in Fig. 7, with the number of planktonic foraminifera
464 and the sea-ice indicator species representing the surface water conditions and the
465 agglutinated/calcareous ratio represents fluctuations in deteriorating bottom water conditions
466 related to the incursion of colder, corrosive BBDW. The grouping of the Atlantic water
467 foraminifera was done following the methods of (Lloyd et al., 2011; Perner et al., 2012, Perner et
468 al., 2011), where *C. neoteretis*, *C. reniforme* and *I. norcrossi* were grouped, to represent the



469 alternation of Atlantic water mass advection to the eastern Baffin Bay. The percentage distribution
 470 of the Atlantic-water group is represented by two curves. One calculated based on the combined
 471 benthic foraminiferal assemblage including both agglutinated and calcareous species and one
 472 without the agglutinated species. This was done in order to evaluate whether increases in this group
 473 are driven by lower abundances of the agglutinated species. Additionally, the species *B.*
 474 *pseudopunctata* and *S. feylingi* were grouped based on their preference of phytoplankton blooms
 475 related to sea-ice margins. The Atlantic-water group is also represented by two different curves.
 476 In Fig. 7, the summary curves from this study, are compared with the estimated mean July air
 477 temperature, derived from regional pollen data from lake cores, using the Modern Analogue
 478 Technique (Gajewski, 2015).



479

480 **Figure 7:** The green and purple curves show the comparison of the agglutinated benthics and calcareous benthics in individuals
 481 per gram of wet sediment, respectively. The sea-ice indicator species curves represent a grouping of the two sea-ice indicator
 482 species *S. feylingi* and *B. pseudopunctata*, shown in percentages including agglutinated species (light blue) and without agglutinated
 483 species (dark blue). *C. neoteretis*, *C. reniforme* and *I. norcrossi* make up the Atlantic water indicator species shown in percentages
 484 including agglutinated species (light red) and without agglutinated species (dark red). The grey bars represent periods of
 485 strengthening of the WGC related to a stronger Atlantic water entrainment. The foraminifera data is compared to North Atlantic
 486 dinocyst taxa (Caron et al., 2019) and the Atlantic water indicator species *I. norcrossi* from core MSM343300, Disko Bugt (Perner
 487 et al., 2012). Additionally, two temperature reconstruction records are included, showing the mean regional July temperature (black
 488 line) from selected sites, constructed by using the modern analogue technique (MAT) on pollen records from lake sediments
 489 (Gajewski, 2015). The light blue shaded areas indicate the regional one standard deviations and the straight vertical line is the long-
 490 term average of the curve.

491 5.1 Early Holocene

492 Several studies based on marine sediment cores from the Baffin Bay and adjacent areas, indicate
 493 that this region was subjected to cold deglacial conditions during the earliest part of the Holocene.



494 A magnetic property study by Caron et al., 2018, carried out on core AMD14-204C, suggests that
495 the homogeneous clayey silts found from 9.2-7.7 ka BP and high values of MDF_{NRM} and magnetic
496 susceptibility, represent a deglacial deposition dominated by glacially-derived material from an
497 ice-distal environment. These results are supported by studies of lake sediments adjacent to the ice
498 stream suggesting that the Upernavik Isstrøm had retreated close to its modern position (Briner et
499 al., 2013).

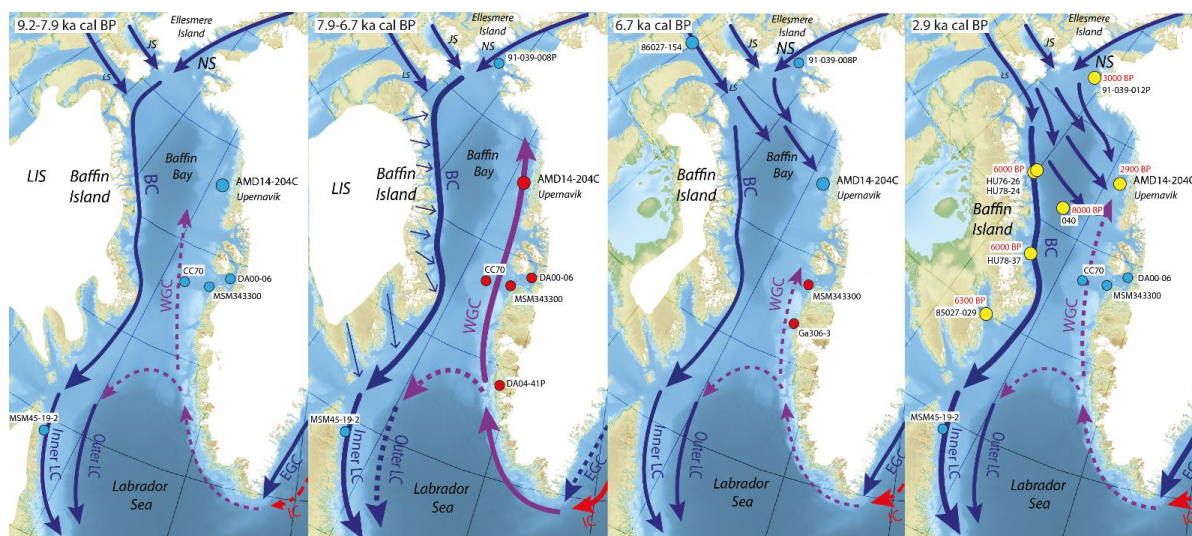
500 The strong influence of cold Polar waters from the Arctic Ocean and extensive sea ice that is
501 suggested by the dominance of *S. feylingi* and the low abundance of the North Atlantic dinocyst
502 taxa (Caron et al., 2019) (Fig. 7), is also observed further southwest of the core AMD14-204C site.
503 In the Labrador Sea (core MSM45-19-2 on Fig. 8), colder conditions were observed during the
504 period 8.9-8.7 ka BP, likely caused by increased advection of colder southward flowing Baffin
505 Bay water masses into the Labrador Current (Lochte et al., 2019). Additionally, the benthic
506 foraminiferal fauna indicate extreme conditions with low food supply and low oxygen conditions
507 related to an extensive sea-ice cover (Lochte et al., 2019) (Fig. 8). These environmental conditions
508 are further supported by dinocyst data from the eastern Baffin Bay west of Disko Bugt (core
509 CC70), indicating cold surface water conditions and extensive sea-ice cover prior to 9.5 ka BP
510 (Gibb et al., 2015). These data also show a shift towards slightly higher salinities and reduced sea
511 ice at ~9.5 ka BP, suggesting a decreasing influence of proximal ablation from the GIS (Gibb et
512 al., 2015).

513 The Disko Bugt in central West Greenland was subjected to similar cold conditions, where
514 sedimentological and benthic foraminiferal data from a marine sediment core near the Jakobshavn
515 Isbræ (core DA00-06) imply that the WGC influence was weaker and highly influenced by
516 significant meltwater influxes already prior to 8.3 ka BP (Lloyd et al., 2005). Additionally, a
517 second study from the Disko Bugt area (core MSM343300) document high abundances of Arctic
518 benthic foraminifera proposing a subsurface cooling, coinciding with increased meltwater
519 injection and sea-ice supply to the surface waters inferred from dinocyst, diatom and alkenone
520 ($\%C_{37:4}$) data (Moros et al., 2016) (Fig. 8).

521 Accordingly, it seems that both surface and subsurface water conditions in the eastern Baffin Bay
522 and adjacent areas were highly affected by waning deglacial conditions in the Early Holocene,
523 with extensive sea-ice cover and ceasing meltwater influence from the marine outlet glaciers from
524 the GIS.



525 Reconstructed mean July temperatures based on pollen records from lake cores, point to colder
526 than average air temperatures during the Early Holocene in both the Eastern Canadian Arctic and
527 Northwest Greenland (a total of 13 sites) (Gajewski, 2015) (Fig. 7). This region was subjected to
528 cold air temperatures prior to 8.2 ka BP, due to the substantial remnants of the Laurentide Ice Sheet
529 (LIS), cooling the adjacent areas and supplying them with meltwater (Renssen et al., 2009). The
530 widespread stratification in West Greenland and in the Baffin Bay due to the increased meltwater
531 supply, is thought to have impeded the deep-water formation in the Labrador Sea (Renssen et al.,
532 2009; Seidenkrantz et al., 2013), resulting in a weaker northward flow of warmer air and water
533 masses (Renssen et al., 2009).



534

535 **Figure 8:** Map showing the oceanographic conditions in the Baffin Bay and Labrador Sea area from 9.2-2.9 ka BP based on this
536 core and other cores from the area; MSM45-19-2 (Lochte et al., 2019), CC70 (Gibb et al., 2015), DA00-06 (Lloyd et al., 2005),
537 DA04-41P (Seidenkrantz et al., 2013), MSM343300 (Perner et al., 2013; Moros et al., 2016), 91-039-008P (Levac et al., 2001),
538 86027-154 (Pieńkowski et al., 2014), 91-039-012P (Levac et al., 2001; Knudsen et al., 2008), HU76-26, HU78-24, HU78-37
539 (Osterman & Nelson et al., 1989), 040 (Aksu, 1983), 85027-029 (Jennings, 1993). Red and blue cores represent relatively warmer
540 and colder conditions, respectively. Solid and dashed arrows indicate stronger and weaker ocean currents, respectively. The straight
541 blue arrows at Baffin Island at 7.9-6.7 ka BP indicate meltwater run-off into the ocean. The yellow cores at 2.9 ka BP indicate
542 sediment cores where a change towards an agglutinated dominated benthic fauna occurred where the red numbers indicate the
543 timing of this transition. Reconstruction of ice sheet extends are modified after Dyke et al., 2004. Abbreviations: LIS = Laurentide
544 Ice Sheet, LS = Lancaster Sound, JS = Jones Sound, NS = Nares Strait, BC = Baffin Current, LC = Labrador Current, IC = Irminger
545 Current, EGC = East Greenland Current, WGC = West Greenland Current.

546 5.2 Mid Holocene

547 The transition to warmer subsurface conditions was initiated around 7.9 ka BP at our study site,
548 marked by the increased abundances of Atlantic water indicator species in the benthic
549 foraminiferal assemblage, coinciding with low abundances of the sea-ice indicator species (Fig.



550 7). Additionally, the appearance of planktonic foraminifera and increase in the North Atlantic
551 dinocyst taxa point to a warming of the surface waters (Caron et al., 2019). The warming of the
552 subsurface waters in the eastern Baffin Bay seem to have persisted for most of the Mid Holocene
553 (7.9-2.9 ka BP); however fluctuations in these conditions are evident. Benthic foraminiferal
554 assemblage composition, and in particular the presence of *C. neoteretis*, infers that this temperature
555 increase was caused by a strengthening of the WGC related to stronger entrainment of Atlantic
556 water masses from 7.9-6.7 ka BP.

557 A concurrent shift in the oceanographic setting has also been identified west of Disko Bugt (core
558 CC70, Fig. 8), where dinocyst assemblages imply increasing SST and further reduction of seasonal
559 sea-ice cover from a strengthened Atlantic water inflow (Gibb et al., 2015). At the same site, the
560 presence of benthic foraminiferal species associated with warm, subsurface water masses from 7.5
561 ka BP was likely also facilitated by decreased meltwater flow from the GIS together with increased
562 inflow of Atlantic water masses (Jennings et al., 2014).

563 Southwest of Disko Bugt (core MSM343300; Fig. 8), evidence of warmer but variable subsurface
564 water conditions is also here linked to an enhancement of warm WGC influence, observed in the
565 benthic foraminiferal record at 7.3-6.2 ka BP (Perner et al., 2012). At core site DA00-06 (Fig. 8)
566 in Disko Bugt itself, a transition towards warmer conditions is marked by an increase in sub-
567 arctic/Atlantic water benthic foraminifera after 7.8 ka cal. BP (Lloyd et al., 2005). This is further
568 supported by the combined multiproxy study (core MSM343300; Fig. 8) by Moros et al., 2016,
569 where low abundances of sea-ice diatoms and dinocysts indicate that also surface water conditions
570 were warmer and relatively stable, with low meltwater influx from the Greenland ice sheet linked
571 to warmer air masses in central West Greenland. A similar decreasing meltwater release from ca
572 7.5 ka BP is also seen further south in Ameralik Fjord near Nuuk (core DA04-41P; Fig. 8)
573 (Seidenkrantz et al., 2013).

574 An oceanographic shift is also observed 7.3 ka BP in the Labrador Sea (core MSM45-19-2) that
575 experienced decreasing surface and bottom water temperatures in connection to a strengthened
576 northward flowing branch of the WGC compared to a weakened westward deflection of the
577 WGC (Lochte et al., 2019; Sheldon et al., 2016). Surface-water reconstructions from the
578 northernmost Baffin Bay (core 91-039-008P) and Newfoundland, i.e. path of the Baffin Current
579 and Labrador Current, propose that increased advection of freshwater from melting Canadian
580 Arctic glaciers strengthened the Baffin Current and Labrador Current (Levac et al, 2001; Solignac



581 et al., 2011). This shift in the flow of the warmer WGC causing an opposite pattern between the
582 western Labrador Sea (core MSM45-19-2) and eastern Baffin Bay/central West Greenland (core
583 CC70, MSM343300, DA00-06, DA04-14P; Fig. 8), was likely fostered by a strengthening of the
584 subpolar gyre (SPG), as a result of the commencement of deep-water formation in the Labrador
585 Sea at 7.5 ka BP (Hillaire-Marcel et al., 2001), after the strong meltwater fluxes from the GIS
586 ceased. Warmer northward advection of Atlantic water masses along the coast of West Greenland,
587 together with a stronger LC flow off eastern Canada, are both patterns typical for a strong SPG
588 (Sheldon et al., 2016). The general Northern Hemisphere warming causing melting of Canadian
589 Arctic glaciers and thus meltwater release to the Baffin Current and the Labrador Current would
590 also strengthen this pattern (Solignac et al., 2011).

591 The generally warmer Mid-Holocene subsurface conditions at AMD14-204C were temporarily
592 interrupted by a drop in the advection of warmer Atlantic water masses at 6.7 ka BP, where the
593 abundances of the Atlantic water benthic foraminiferal indicator species decreased temporarily.
594 Caron et al. (2018) observed a high IRD concentration at 6.7 ka (Fig. 6). It also coincides with low
595 North Atlantic dinocyst taxa abundances (Caron et al., 2019), high sedimentations rates and a peak
596 in the Ca/Ti and Ca/Sr elemental ratios together with high abundances of sea-ice indicator species
597 in our study, suggesting overall cold surface and subsurface water conditions. Palaeozoic
598 limestones and dolostones are commonly found at the flanks of Nares Strait and Lancaster Sounds
599 in the northern part of Baffin Bay (Hiscott et al., 1989), whereas the northwestern coast of
600 Greenland consists of fold belts consisting of reworked Archean basement rocks (mainly gneisses)
601 interfolded with overlying sediment sequences (marble, schist and quartzite) and granitic
602 intrusions (Henriksen, 2005). Older carbonate-rich layers are found in the Baffin Bay marine
603 deposits as a result of ice-rafting in the northern Baffin Bay, which are then exported southward
604 with the BC (Andrews et al., 2011). The IRD found in this core were presumably exported from
605 the Nares Strait or Lancaster Sound by increased incursion of Polar water masses from the Arctic
606 Ocean, transported southward by the BC, after which it re-circulated eastwards to the northeastern
607 Baffin Bay, as has previously been suggested for older marine records (Andrews et al., 2011;
608 Jackson et al., 2017). Adding to this, the eastward transport of IRD was possibly fostered by a
609 strengthening of the northwesterly winds due to the decrease in high latitude insolation after 7 ka
610 BP (Renssen et al., 2005). Supporting this, the Lancaster Sound was subjected to full cold Arctic
611 conditions with enhanced sea-ice cover from 7.2-6.5 ka BP (Pieńkowski et al., 2014), and the
612 Northern Baffin Bay experienced colder summer surface water temperatures (Fig. 8, core 91-039-



613 008P). However, in Disko Bugt there are no signs of surface and subsurface water cooling (Fig. 7)
614 (Moros et al., 2016; Perner et al., 2012; Erbs-Hansen et al., 2013), suggesting a local cooling of
615 the northern Baffin Bay.

616 A return to a period with warmer subsurface waters in the eastern Baffin Bay is facilitated by a re-
617 strengthening of the WGC and Atlantic water entrainment from 6.2-5.3 ka BP inferred by the
618 reappearance of high abundances in the Atlantic water indicator species in our study. The low
619 abundance of the Atlantic water indicator species *I. norcrossi* at around 6 ka BP in core
620 MSM343300 (Fig. 7) implies a cooling of the subsurface waters. However, the low abundance of
621 *I. norcrossi* here might have been caused by other factors such as changes in nutrients availability,
622 since other records in the Disko Bugt/central West Greenland area do not record a prominent
623 subsurface water cooling at that time (Erbs-Hansen et al., 2013; Jennings et al., 2014; Lloyd et al.,
624 2005).

625 Another drop in the WGC strength is evident at 5.3 ka BP at our study site, allowing the incursion
626 of both Polar surface waters and BBDW, as deduced by the high agglutinated/calcareous ratio
627 observed in this study. This event corresponds to the onset of a general decrease in the July air
628 temperatures over the Eastern Canadian Arctic (Fig. 7) (Gajewski, 2015), followed by generally
629 stable air temperatures above average until ca. 2.5 ka BP. The two periods with strong WGC flow
630 associated by enhanced Atlantic water incursion around 7.4 ka BP and again at 6.0 ka BP, seem to
631 occur simultaneously with increasing July air temperatures over the Eastern Canadian Arctic, (Fig.
632 7) (Gajewski, 2015).

633 The general subsurface conditions in the eastern Baffin Bay and West Greenland during the Mid
634 Holocene from 7.9 ka BP to ca. 2.9 ka BP are thus affected by overall warmer conditions, related
635 to a strong northward flow of Atlantic water masses, with minimal influx of meltwater from the
636 GIS. These warmer conditions coincide with the Holocene Thermal Maximum (HTM)
637 corresponding to the timing of the eastern Canadian Arctic (Kaufman et al., 2004), observed in
638 Greenland ice cores with peak warming at 7-6 ka BP (e.g. Dahl-Jensen et al., 1998; Johnsen et al.,
639 2001). The delayed onset of the HTM is in the eastern Canadian Arctic and eastern Baffin Bay
640 associated with the final collapse of the LIS (Kaufman et al., 2004).

641 **5.3 The Late Holocene**

642 The warm surface and subsurface conditions of the eastern Baffin Bay during the HTM, was
643 followed by a period of sudden deteriorating bottom-water conditions, as inferred from the abrupt



644 increase in the agglutinated/calcareous foraminiferal species ratio together with the presence of
645 few Atlantic water indicator species and low abundances of planktonic foraminifera, attributed an
646 enhanced BBDW advection to the core site. The green record in Fig. 7 shows that the distribution
647 of agglutinated species does not increase significantly at the transition to this ecozone, whereas the
648 abundance of the calcareous species (purple curve Fig. 7) drops abruptly. This implies that the
649 increase in the agglutinated/calcareous ratio is not an artefact of a low abundance of agglutinated
650 species down core due to bad preservation, but that it is in fact attributed a true oceanographic
651 change. A marine sediment core from the southern Nares Strait, also recorded this abrupt shift
652 towards a benthic foraminiferal fauna dominated by agglutinated species around 3.0 ka BP
653 (Knudsen et al., 2008). The authors also explained this by an enhanced influence of Arctic Ocean
654 water masses. Several studies from various parts of the Baffin Bay have in fact documented this
655 increased Arctic Ocean water incursion but at various times with the earliest at 8 ka BP and the
656 latest at ca. 3 ka BP (Aksu, 1983; Jennings, 1993; Osterman et al., 1985; Osterman & Nelson,
657 1989). Based on previous studies together with findings in our study, it can be deduced that the
658 timing of the incursion of high saline, cold CO₂-rich Arctic water masses occurred in the deeper
659 central part of the Baffin Bay first and later in the shallower coastal areas, as suggested by
660 (Knudsen et al., 2008).

661 The cold BBDW does not reach the Disko Bugt at water depths greater than 300 m today
662 (Andersen, 1981); however, cold conditions are also evident here. (Perner et al., 2012) recorded
663 an increase in the abundances of agglutinated and Arctic water foraminifera at 3.5 ka BP, and they
664 suggested that this was caused by a freshening of the bottom waters due to an increased
665 entrainment of the EGC into the WGC, and a less significant Atlantic water entrainment. This
666 agrees well with the low abundances of Atlantic water indicator species found in our study,
667 possibly ascribed to a weaker AMOC. Concurrently, also the surface waters in Disko Bugt were
668 cold in the Late Holocene (Moros et al., 2016), suggesting a general cooling trend of the subsurface
669 and surface water temperatures in West Greenland (Andresen et al., 2011; Erbs-Hansen et al.,
670 2013; Lloyd et al., 2007; Seidenkrantz et al., 2007; Seidenkrantz et al., 2008; Lloyd, 2006). An
671 increased outflow of Polar waters from the Arctic Ocean, resulting in a strengthening and cooling
672 of the Baffin Current and Labrador Current is documented in cores CC70 and MSM45-19-2 from
673 the Labrador Shelf (Fig. 8), where dinocyst and benthic foraminiferal assemblages document a
674 surface and subsurface water cooling after 3 ka BP (Gibb et al., 2015; Lochte et al., 2019).
675 However, in the southwestern Labrador Sea, surface and subsurface water ameliorations are



676 recorded by dinocyst and benthic foraminifera data around 2.8 ka BP (Sheldon et al., 2016;
677 Solignac et al., 2011), indicating an increasing influence from warmer Atlantic water masses
678 versus the colder LC water masses, due to a northward placement of the frontal zone between the
679 Gulfstream and the LC (Sheldon et al., 2016), thus implying that the outflow of cold Arctic Ocean
680 waters did not reach the southeastern Labrador Sea.

681 The general cooling trend recorded in the marine records described here, is also observed in the
682 pollen records from the Eastern Canadian Arctic and North Greenland with July air temperatures
683 being lower than average starting at 1.5 and 2.8 ka BP, respectively (Fig. 7) (Gajewski, 2015).
684 This general cooling trend observed in vast areas of the North Atlantic in the late Holocene
685 corresponds to the Neoglaciation, linked to the initiation of readvances in many of the glaciers and
686 ice streams in West Greenland, including the Upernavik Isstrøm (Briner et al., 2013). An advance
687 of the Upernavik Isstrøm could explain the higher IRD counts in this ecozone, related to increased
688 iceberg calving. However, it seems that the onset of the cold subsurface conditions in the eastern
689 Baffin Bay recorded in our study is not fully synchronous with the change towards colder summer
690 air temperatures in the Eastern Canadian Arctic. Nevertheless, the onset of the cold Neoglacial in
691 the eastern Baffin Bay resembles the onset of colder air temperatures recorded in North Greenland,
692 possibly related to the enhanced inflow of the cold Arctic water masses, subjecting the eastern
693 Baffin Bay to high latitude conditions alike the conditions in the North Greenland.

694 Superimposed on the Neoglacial cooling, shorter temporal subsurface water ameliorations are
695 evident in the eastern Baffin Bay, here associated to a re-strengthening in the WGC and Atlantic
696 water inflow, centred at 1.6 ka BP, 1.2 ka BP and 0.8 ka BP. These peaks in the Atlantic water
697 group are seen in both curves representing the percentage distribution of this group. However, the
698 percentages calculated without including the agglutinated species are quite high and not reliable
699 since the total sum of calcareous benthic foraminifera here are too low to be statistically significant
700 for interpretations.

701 In Disko Bugt the late Holocene is characterized by short-lived warmings of both the surface and
702 subsurface waters, related to an enhanced IC advection (Andresen et al., 2011; Lloyd, 2006; Moros
703 et al., 2006; Moros et al., 2016; Perner et al., 2012). Also records from the Labrador Sea have
704 documented these warmings from 2.0 to 1.5 ka indicated by fluctuating lengths of the sea-ice
705 seasons (Lochte et al., 2019), coinciding with shorter warmings found in the Placentia Bay in
706 Newfoundland (Solignac et al., 2011), and in the shelf waters of East Greenland (Jennings et al.,



707 2002). These widespread late Holocene centennial scale climate fluctuations were presumably
708 facilitated by fluctuations in the atmospheric circulation pattern over the North Atlantic,
709 controlling the strength of the northwesterly winds. However, a higher temporal resolution is
710 needed in order to fully resolve these short-term climatic fluctuations documented in this study
711 and other studies from the North Atlantic.

712 **6 Conclusion**

713 The presented multiproxy study based on benthic foraminiferal assemblage analysis and X-ray
714 fluorescence data, document several climatic and oceanographic changes in eastern Baffin Bay
715 during the Holocene:

- 716 1. The eastern Baffin Bay was subjected to cold deglacial conditions in the Early Holocene
717 (9.2-7.9 ka BP) associated with an extensive sea-ice cover and meltwater inflows supplied
718 by the melting of the Greenland Ice Sheet. Subsurface water conditions are characterized
719 by a very low benthic foraminiferal species diversity and the coeval low abundances of
720 Atlantic water indicator species reflecting a low entrainment of Atlantic water into the West
721 Greenland Current.
- 722 2. A transition towards warmer subsurface water conditions is evident at the onset of the Mid
723 Holocene (7.9 ka BP) encompassing the Holocene Thermal Maximum, where the eastern
724 Baffin Bay was subjected to a strengthening in the West Greenland Current flow related to
725 an increased Atlantic water incursion and ceasing meltwater influxes from the Greenland
726 Ice Sheet. The ameliorating conditions found here are linked to a widespread
727 oceanographic shift in the North Atlantic, due to the commencement of deep-water
728 formation in the Labrador Sea.
- 729 3. The general ameliorating conditions found in the mid Holocene were interrupted by a
730 cooling period centred at 6.7 ka BP, deduced from high abundances in the sea-ice indicator
731 species and high IRD counts, where the latter presumably originated from the gateways of
732 the Canadian Arctic Archipelago inferred by the high Ca-content observed in the XRF data.
733 This cold period is ascribed to a weakening of the subpolar gyre, facilitating a weakening
734 of the northward flowing Atlantic water masses along the West Greenland coast.
- 735 4. Evidence of enhanced inflow of the cold, corrosive and dense Baffin Bay Deep Water is
736 documented at 5.3 ka BP, reflected by low abundances of the calcareous benthic species
737 together with a decrease in the abundances of the Atlantic water indicator species. This is
738 concurrent with a drop in the estimated July air temperatures found in the Eastern Arctic.



739 5. A drastic shift in the ocean circulation system occurred around 2.9 ka BP, ascribed to the
740 onset of the Neoglacial cooling. The eastern Baffin Bay were subjected to an enhanced
741 southward inflow of cold, corrosive and dense Baffin Bay Deep Water, recorded by the
742 domination of agglutinated benthic foraminifera.

743 6. Short-lived bottom water warmings superimposed on the Neoglacial cooling, characterize
744 the latest part of the Holocene, possibly facilitated by fluctuations in the atmospheric
745 circulation system affecting the strength of the northwesterly winds.

746

747 **7 Author contribution**

748 M-SS developed the research idea. KEH conducted the benthic foraminiferal assemblage analysis
749 with major contributions from M-SS. LW carried out the seven additional radiocarbon. JG
750 provided four radiocarbon datings. CP performed the age modelling of the core. KEH prepared the
751 manuscript with contributions from all co-authors.

752

753 **8 Competing interests**

754 Author M-SS is co-editor-in-chief of the journal.

755

756 **9 Acknowledgment**

757 We are grateful to the captain, crew and scientific party of the CCGS *Amundsen* 2014 expedition
758 for their work in retrieval of sediment core AMD14-204C. Additionally, we would like to thank
759 the ERC STG ICEPROXY 203441 for the financial support for the ship time. We also thank
760 Guillaume Massé for the opportunity to work on the marine sediment core AMD14-204C. We also
761 wish to thank Eleanor Georgiadis, Philippe Martinez, and Isabelle Billy for running the x-ray
762 fluorescence spectroscopy of the core at the EPOC laboratory in Bordeaux, and for composing
763 these datasets. We also thank Myriam Caron for the dynocyst, IRD and grain size data set. This
764 study is a part of the “G-Ice” project, funded by the Danish Council for Independent Research
765 (grant no. 7014-00113B/FNU) to MSS.

766

767 **10 References**

768 Aksenov, Y., Bacon, S., Coward, A. C. and Holliday, N. P.: Polar outflow from the Arctic Ocean: A high resolution
769 model study, *J. Mar. Syst.*, 83(1–2), 14–37, doi:10.1016/j.jmarsys.2010.06.007, 2010.
770 Aksu, A.: Late Quaternary Stratigraphy, Palaeoenvironmentology and Sedimentation History of Baffin Bay and
771 Davis Strait, Dallahouse University., 1981.
772 Aksu, A.: Holocene and Pleistocene dissolution cycles in deepsea cores of Baffin Island and Davies Strait:



- 773 Paleooceanographic implications, *Mar. Geol.*, 53, 331–348, 1983.
- 774 Andersen, O. G. N.: The annual cycle of temperature, salinity, currents and water masses in Disko Bugt and adjacent
775 waters, West Greenland, *Meddelelser om Grønland, Biosci.*, 5, 1–36, 1981.
- 776 Andresen, C. S., McCarthy, D. J., Dylmer, C. V., Seidenkrantz, M. S., Kuijpers, A. and Lloyd, J. M.: Interaction
777 between subsurface ocean waters and calving of the Jakobshavn Isbræ during the late Holocene, *Holocene*, 21(2),
778 211–224, doi:10.1177/0959683610378877, 2011.
- 779 Andresen, C. S., Kjeldsen, K. K., Harden, B., Nørgaard-pedersen, N. and Kjær, K. H.: Outlet glacier dynamics and
780 bathymetry at Upernavik, *GEUS Bullitin*, 31(August 2014), 81–84, 2014.
- 781 Andrews, J. T., Eberl, D. D. and Scott, D.: Surface (sea floor) and near-surface (box cores) sediment mineralogy in
782 Baffin Bay as a key to sediment provenance and ice sheet variations, *Can. J. Earth Sci.*, 48, 1307–1328,
783 doi:10.1139/e11-021, 2011.
- 784 Anon: NSIDC (National Snow and Ice Data Centre), Atlas Cryosph. [online] Available from:
785 ftp://sidacs.colorado.edu/DATASETS/NOAA/G02135/north/monthly/shapefiles/shp_median/, 2019.
- 786 Bahr, A., Lamy, F., Arz, H., Kuhlmann, H. and Wefer, G.: Late glacial to Holocene climate and sedimentation
787 history in the NW Black Sea, *Mar. Geol.*, 214(4), 309–322, doi:10.1016/j.margeo.2004.11.013, 2005.
- 788 Bourke, R. H. & Paquette, R. G.: Formation of Baffin Bay bottom and deep waters, in *Deep convection and deep
789 water formation in the oceans*, edited by J. C. Chu, P. C. & Gascard, pp. 135–155, Elsevier, Amsterdam., 1991.
- 790 Briner, J. P., Håkansson, L. and Bennike, O.: The deglaciation and neoglaciation of upernavik isstrøm, greenland,
791 *Quat. Res. (United States)*, 80(3), 459–467, doi:10.1016/j.yqres.2013.09.008, 2013.
- 792 Buch, E.: A monograph on the physical oceanography of the Greenland waters, Royal Danish Administration of
793 Navigation and Hydrography, Copenhagen., 1994.
- 794 Bunker, A. F.: Computations of Surface Energy Flux and Annual Air–Sea Interaction Cycles of the North Atlantic
795 Ocean, *Mon. Weather Rev.*, 104(9), 1122–1140, doi:10.1175/1520-0493(1976)104<1122:cosefa>2.0.co;2, 1976.
- 796 Calvert, S. E. and Pedersen, T. F.: Geochemistry of Recent oxic and anoxic marine sediments: Implications for the
797 geological record, *Mar. Geol.*, 113(1–2), 67–88, doi:10.1016/0025-3227(93)90150-T, 1993.
- 798 Caron, M., St-Onge, G., Montero-Serrano, J. C., Rochon, A., Georgiadis, E., Giraudeau, J. and Massé, G.: Holocene
799 chronostratigraphy of northeastern Baffin Bay based on radiocarbon and palaeomagnetic data, *Boreas*, 48(1), 147–
800 165, doi:10.1111/bor.12346, 2018.
- 801 Caron, M., Rochon, A., Carlos, J., Serrano, M. and Onge, G. S. T.: Evolution of sea-surface conditions on the
802 northwestern Greenland margin during the Holocene, *J. Quat. Sci.*, 1–12, doi:10.1002/jqs.3146, 2019.
- 803 Collin, A. E.: Oceanographic observations in Nares Strait, northern Baffin Bay 1963, 1964, Dartmouth, NS., 1965.
- 804 Cuny, J., Rhines, P. B., Niiler, P. P. and Bacon, S.: Labrador Sea Boundary Currents and the Fate of the Irminger
805 Sea Water, *J. Phys. Oceanogr.*, 32, 627–647, doi:10.1175/1520-0485(2002)032<0627:LSBCAT>2.0.CO;2, 2002.
- 806 Dahl-Jensen, D., Mosegaard, K., Gundestrup, N., Clow, G. D., Johnsen, S. J., Hansen, A. W. and Balling, N.: Past
807 temperatures directly from the Greenland Ice Sheet, *Science (80-.)*, 282, 268–271,
808 doi:10.1126/science.282.5387.268, 1998.
- 809 Drinkwater, K. F.: Atmospheric and oceanic variability in the northwest Atlantic during the 1980s and early 1990s,
810 *J. Northwest Atl. Fish. Sci.*, 18, 77–97, doi:10.2960/J.v18.a6, 1996.
- 811 Dunbar, M. & Dunbar, M. J.: The history of the North Water, *Proc. R. Soc. Edinburgh, Sect. B Biol. Sci.*, 72(1),
812 231–241, 1972.
- 813 England, J., Atkinson, N., Bednarski, J., Dyke, A. S., Hodgson, D. A. and Ó Cofaigh, C.: The Inuitian Ice Sheet:
814 configuration, dynamics and chronology, *Quat. Sci. Rev.*, 25(7–8), 689–703, doi:10.1016/j.quascirev.2005.08.007,
815 2006.
- 816 Erbs-Hansen, Dorthe Reng Knudsen, K. L., Olsen, J., Lykke-Andersen, H., Underbjerg, J. A. and Sha, L.:
817 Paleooceanographical development off Sisimiut, West Greenland, during the mid- and late Holocene: A multiproxy
818 study, *Mar. Micropaleontol.*, 102, 79–97, doi:10.1016/j.marmicro.2013.06.003, 2013.
- 819 Funder, S. (ed. .: Late Quaternary stratigraphy and glaciology in the Thule area, Northwest Greenland, *Meddelelser
820 om Grønland, Geosci.*, 22, 1–63, 1990.
- 821 Gajewski, K.: Quantitative reconstruction of Holocene temperatures across the Canadian Arctic and Greenland,
822 *Glob. Planet. Change*, 128, 14–23, doi:10.1016/j.gloplacha.2015.02.003, 2015.



- 823 Georgiadis, E., Giraudeau, J., Martinez, P., Lajeunesse, P., St-Onge, G., Schmidt, S. and Massé, G.: Deglacial to
824 postglacial history of Nares Strait, Northwest Greenland: A marine perspective from Kane Basin, *Clim. Past*, 14(12),
825 1991–2010, doi:10.5194/cp-14-1991-2018, 2018.
- 826 Gibb, O. T., Steinhauer, S., Fréchette, B., de Vernal, A. and Hillaire-Marcel, C.: Diachronous evolution of sea
827 surface conditions in the Labrador sea and Baffin Bay since the last deglaciation, *Holocene*, 25(12), 1882–1897,
828 doi:10.1177/0959683615591352, 2015.
- 829 Giraudeau, J., Georgiadis, E., Caron, M., Martinez, P., Saint-Onge, G., Billy, I., Lebleu, P., Ther, O. and Massé, G.:
830 A high-resolution elemental record of post-glacial lithic sedimentation in Upernavik Trough, western Greenland:
831 history of ice-sheet dynamics and ocean circulation changes over the last 9 100 years, *Paleoceanogr.*
832 *Paleoclimatology*, 1–37, n.d.
- 833 Gustafsson, M. and Nordberg, K.: Living (stained) benthic foraminiferal response to primary production and
834 hydrography in the deepest part of the Gullmar Fjord, Swedish West Coast, with comparisons to Hoglund's 1927
835 material, *J. Foraminifer. Res.*, 31, 2–11, doi:10.2113/0310002, 2001.
- 836 Henriksen, N.: Geological History of Greenland - Four billion years of Earth evolution, Geological Survey of
837 Denmark and Greenland (GEUS), Copenhagen., 2005.
- 838 Hillaire-Marcel, C., DeVernal, A., Bilodeau, G. and Weaver, A. J.: Absence of deep-water formation in the
839 Labrador Sea during the last interglacial period, *Nature*, 410(6832), 1073–1077, 2001.
- 840 Hiscott, R. N., Aksu, A. E. and Nielsen, O. B.: Provenance and Dispersal Patterns, Pliocene-Pleistocene Section at
841 Site 645, Baffin Bay, in *Proceedings of the Ocean Drilling Program, 105 Scientific Results*, pp. 31–52., 1989.
- 842 Holland, D. M., Thomas, R. H., De Young, B., Ribergaard, M. H. and Lyberth, B.: Acceleration of Jakobshavn Isbr
843 triggered by warm subsurface ocean waters, *Nat. Geosci.*, 1(10), 659–664, doi:10.1038/ngeo316, 2008.
- 844 Jackson, R., Carlson, A. E., Hillaire-Marcel, C., Wacker, L., Vogt, C. and Kucera, M.: Asynchronous instability of
845 the North American-Arctic and Greenland ice sheets during the last deglaciation, *Quat. Sci. Rev.*, 164, 140–153,
846 doi:10.1016/j.quascirev.2017.03.020, 2017.
- 847 Jennings, A. E.: the Quaternary History of Cumberland Sound, Southeastern Baffin-Island - the Marine Evidence,
848 *Geogr. Phys. Quat.*, 47(1), 21–42, 1993.
- 849 Jennings, A. E. and Helgadottir, G.: Foraminiferal assemblages from the fjords and shelf of eastern Greenland, *J.*
850 *Foraminifer. Res.*, 24, 123–144, 1994.
- 851 Jennings, A. E., Andrews, J. T., Knudsen, K. L., Hansen, C. V. and Hald, M.: A mid-Holocene shift in Arctic sea-ice
852 variability on the East Greenland Shelf, *Holocene*, 12, 49–58, doi:10.1191/0959683602hl519rp, 2002.
- 853 Jennings, A. E., Weiner, N. J. and Helgadottir, G.: Modern foraminiferal faunas of the southwestern to northern
854 Iceland shelf: Oceanographic and environmental controls, *J. Foraminifer. Res.*, 34(3), 180–207,
855 doi:10.2113/34.3.180, 2004.
- 856 Jennings, A. E., Sheldon, C., Cronin, T., Francus, P., Stoner, J. S. and Andrews, J.: The Holocene History of Nares
857 Strait, *Oceanography*, 24(3), 26–41, 2011.
- 858 Jennings, A. E., Ó Cofaigh, C., Ortiz, J. D., De Vernal, A., Dowdeswell, J. A., Kilfeather, A., Walton, M. E. and
859 Andrews, J.: Paleoenvironments during Younger Dryas-Early Holocene retreat of the Greenland Ice Sheet from
860 outer Disko Trough, central west Greenland, *J. Quat. Sci.*, 29(1), 27–40, doi:10.1002/jqs.2652, 2014.
- 861 Jennings, A. E., Andrews, J. T., Ó Cofaigh, C., Onge, G. S., Sheldon, C., Belt, S. T., Cabedo-Sanz, P. and Hillaire-
862 Marcel, C.: Ocean forcing of Ice Sheet retreat in central west Greenland from LGM to the early Holocene, *Earth*
863 *Planet. Sci. Lett.*, 472, 1–13, doi:10.1016/j.epsl.2017.05.007, 2017.
- 864 Jennings, A. E., Andrews, J. T., Ó Cofaigh, C., St-Onge, G., Belt, S., Cabedo-Sanz, P., Pearce, C., Hillaire-Marcel,
865 C. and Calvin Campbell, D.: Baffin Bay paleoenvironments in the LGM and HS1: Resolving the ice-shelf question,
866 *Mar. Geol.*, 402, 5–16, doi:10.1016/j.margeo.2017.09.002, 2018.
- 867 Jennings, A. E., Andrews, J. T., Oliver, B., Walczak, M. and Mix, A.: Retreat of the Smith Sound Ice Stream in the
868 Early Holocene, *Boreas*, 1–16, doi:10.1111/bor.12391, 2019.
- 869 Johnsen, S. J., Dahl-Jensen, D., Gundestrup, N., Steffensen, J. P., Clausen, H. B., Miller, H., Masson-Delmotte, V.,
870 Sveinbjörnsdóttir, A. E. and White, J.: Oxygen isotope and palaeotemperature records from six Greenland ice-core
871 stations: Camp Century, Dye-3, GRIP, GISP2, Renland and NorthGRIP, *J. Quat. Sci.*, 16, 299–307,
872 doi:10.1002/jqs.622, 2001.



- 873 Jones, E. P. and Anderson, L. G.: Is the global conveyor belt threatened by arctic ocean fresh water outflow?, in
874 Arctic-Subarctic Ocean Fluxes: Defining the Role of the Northern Seas in Climate, edited by R. R. Dickson, J.
875 Meincke, and P. Rhines, pp. 385–404, Springer., 2008.
- 876 Kaufman, D. S., Ager, T. A., Anderson, N. J., Anderson, P. M., Andrews, J. T., Bartlein, P. J., Brubaker, L. B.,
877 Coats, L. L., Cwynar, L. C., Duvall, M. L., Dyke, A. S., Edwards, M. E., Eisner, W. R., Gajewski, K., Geirsdóttir,
878 A., Hu, F. S., Jennings, A. E., Kaplan, M. R., Kerwin, M. W., Lozhkin, A. V., MacDonald, G. M., Miller, G. H.,
879 Mock, C. J., Oswald, W. W., Otto-Bliesner, B. L., Porinchu, D. F., Rühland, K., Smol, J. P., Steig, E. J. and Wolfe,
880 B. B.: Holocene thermal maximum in the western Arctic (0-180°W), *Quat. Sci. Rev.*, 23, 529–560,
881 doi:10.1016/j.quascirev.2003.09.007, 2004.
- 882 Knudsen, K. L. and Seidenkrantz, M.-S.: *Stainforthia feylingi* new species from arctic to subarctic environments,
883 previously recorded as *Stainforthia schreibersiana*, *Cushman Found. Foraminifer. Res. Spec. Publ.*, 32, 5–13, 1994.
- 884 Knudsen, K. L., Conradsen, K., Heier-Nielsen, S. and Seidenkrantz, M. S.: Palaeoenvironments in the Skagerrak-
885 Kattegat basin in the eastern North Sea during the last deglaciation, *Boreas*, 25(2), 65–78, doi:10.1111/j.1502-
886 3885.1996.tb00836.x, 1996.
- 887 Knudsen, K. L., Stabell, B., Seidenkrantz, M. S., Eiríksson, J. and Blake, W.: Deglacial and Holocene conditions in
888 northernmost Baffin Bay: Sediments, foraminifera, diatoms and stable isotopes, *Boreas*, 37(3), 346–376,
889 doi:10.1111/j.1502-3885.2008.00035.x, 2008.
- 890 Korsun, S. and Hald, M.: Modern Benthic Foraminifera off Novaya Zemlya Tidewater Glaciers, Russian Arctic,
891 *Arct. Alp. Res.*, 30(1), doi:10.2307/1551746, 1998.
- 892 Korsun, S. and Hald, M.: Seasonal dynamics of benthic foraminifera in a glacially fed fjord of Svalbard, *European*
893 *Arctic, J. Foraminifer. Res.*, 30(4), 251–271, doi:10.2113/0300251, 2000.
- 894 Landry M.R. and Stukel M.R. Brzezinski M.A. Krause J.W., B. R. M. B. K. A. F. P. G. R.: *Journal of Geophysical*
895 *Research : Oceans, J. Geophys. Res. Ocean.*, 120(7), 4654–4669, doi:10.1002/2015JC010829.Received, 2015.
- 896 Levac, E., De Vernal, A. and Blake, W.: Sea-surface conditions in northernmost Baffin Bay during the Holocene:
897 Palynological evidence, *J. Quat. Sci.*, 16(4), 353–363, doi:10.1002/jqs.614, 2001.
- 898 Lloyd, J., Moros, M., Perner, K., Telford, R. J., Kuijpers, A., Jansen, E. and McCarthy, D.: A 100 yr record of ocean
899 temperature control on the stability of Jakobshavn Isbrae, West Greenland, *Geology*, 39(9), 867–870,
900 doi:10.1130/G32076.1, 2011.
- 901 Lloyd, J. M.: Late Holocene environmental change in Disko Bugt, west Greenland: Interaction between climate,
902 ocean circulation and Jakobshavn Isbrae, *Boreas*, 35, 35–49, doi:10.1111/j.1502-3885.2006.tb01111.x, 2006a.
- 903 Lloyd, J. M.: Modern distribution of benthic foraminifera from Disko Bugt, West Greenland, *J. Foraminifer. Res.*,
904 36, 315–331, doi:10.2113/gsjfr.36.4.315, 2006b.
- 905 Lloyd, J. M., Park, L. A., Kuijpers, A. and Moros, M.: Early Holocene palaeoceanography and deglacial chronology
906 of Disko Bugt, West Greenland, *Quat. Sci. Rev.*, 24(14–15), 1741–1755, doi:10.1016/j.quascirev.2004.07.024,
907 2005.
- 908 Lloyd, J. M., Kuijpers, A., Long, A., Moros, M. and Park, L. A.: Foraminiferal reconstruction of mid- to late-
909 Holocene ocean circulation and climate variability in Disko Bugt , West Greenland, *The Holocene*, 17(8), 1079–
910 1091, doi:10.1177/0959683607082548, 2007.
- 911 Locarnini, R. A., Mishonov, A. V., Antonov, J. I., Boyer, T. P., Garcia, H. E., Baranova, O. K., Zweng, M. M.,
912 Paver, C. R., Reagan, J. R., Johnson, D. R., Hamilton, M. and Seidov, D.: *WORLD OCEAN ATLAS 2013:*
913 *Temperature Volume 1*, edited by A. Mishonov Technical Ed., NOAA Atlas NESDIS 73., 2013.
- 914 Lochte, A. A., Repschläger, J., Seidenkrantz, M.-S., Kienast, M., Blanz, T. and Schneider, R. R.: Holocene water
915 mass changes in the Labrador Current, *The Holocene*, 2019.
- 916 Melling, H., Gratton, Y., Ingram, G., Melling, H., Gratton, Y. and Ingram, G.: Ocean circulation within the North
917 Water polynya of Baffin Bay Ocean Circulation within the North Water Polynya of Baffin Bay, , 39(3), 301–325,
918 doi:10.1080/07055900.2001.9649683, 2010.
- 919 Mertz, G., Narayanan, S., Helbig, J.: The freshwater transport of the labrador current, *Atmos. - Ocean*, 31(2), 281–
920 295, doi:10.1080/07055900.1993.9649472, 1993.
- 921 Morlighem, M., Williams, C. N., Rignot, E., An, L., Arndt, J. E., Bamber, J. L., Catania, G., Chauché, N.,
922 Dowdeswell, J. A., Dorschel, B., Fenty, I., Hogan, K., Howat, I., Hubbard, A., Jakobsson, M., Jordan, T. M.,



- 923 Kjeldsen, K. K., Millan, R., Mayer, L., Mouginot, J., Noël, B. P. Y., O’Cofaigh, C., Palmer, S., Rysgaard, S.,
924 Seroussi, H., Siegert, M. J., Slabon, P., Straneo, F., van den Broeke, M. R., Weinrebe, W., Wood, M. and
925 Zinglarsen, K. B.: BedMachine v3: Complete Bed Topography and Ocean Bathymetry Mapping of Greenland From
926 Multibeam Echo Sounding Combined With Mass Conservation, *Geophys. Res. Lett.*, doi:10.1002/2017GL074954,
927 2017.
- 928 Moros, M., Jensen, K. G. and Kuijpers, A.: Mid- to late-Holocene hydrological and climatic variability in Disko
929 Bugt, central West Greenland, Holocene, doi:10.1191/0959683606h1933rp, 2006.
- 930 Moros, M., Lloyd, J. M., Jennings, A. E., Krawczyk, D., Witkowski, A., Blanz, T., Kuijpers, A., Ouellet-Bernier,
931 M.-M., de Vernal, A., Schneider, R., Perner, K. and Jansen, E.: Surface and sub-surface multi-proxy reconstruction
932 of middle to late Holocene palaeoceanographic changes in Disko Bugt, West Greenland, *Quat. Sci. Rev.*, 132, 146–
933 160, doi:10.1016/j.quascirev.2015.11.017, 2016.
- 934 Nagler, T., Rott, H., Hetzenecker, M., Wuite, J. and Potin, P.: The Sentinel-1 mission: New opportunities for ice
935 sheet observations, *Remote Sens.*, doi:10.3390/rs70709371, 2015.
- 936 Osterman, L. E. and Nelson, A. R.: Latest Quaternary and Holocene paleoceanography of the eastern Baffin Island
937 continental shelf, Canada: benthic foraminiferal evidence, *Can. J. Earth Sci.*, 26, 2236–2248, doi:10.1139/e89-190,
938 1989.
- 939 Osterman, L. E., Miller, G. H. and Stravers, J. A.: Late and mid- Foxe glaciation of southern Baffin Island, in
940 Quaternary Environments, Eastern Canadian Arctic, Baffin Bay and Western Greenland, edited by J. T. Andrews,
941 pp. 520–545, Allen & Unwin, London, 1985.
- 942 Patterson, R. T., Guilbault, J. P. and Thomson, R. E.: Oxygen level control on foraminiferal distribution in
943 Effingham Inlet, Vancouver Island, British Columbia, Canada, *J. Foraminifer. Res.*, 30, 321–335,
944 doi:10.2113/0300321, 2000.
- 945 Perner, K., Moros, M., Lloyd, J. M., Kuijpers, A., Telford, R. J. and Harff, J.: Centennial scale benthic foraminiferal
946 record of late Holocene oceanographic variability in Disko Bugt, West Greenland, *Quat. Sci. Rev.*, 30, 2815–2826,
947 doi:10.1016/j.quascirev.2011.06.018, 2011.
- 948 Perner, K., Moros, M., Jennings, A., Lloyd, J. M. and Knudsen, K. L.: Holocene palaeoceanographic evolution off
949 West Greenland, Holocene, 23(3), 374–387, doi:10.1177/0959683612460785, 2012.
- 950 Pieńkowski, A. J., England, J. H., Furze, M. F. A., MacLean, B. and Blasco, S.: The late Quaternary environmental
951 evolution of marine Arctic Canada: Barrow Strait to Lancaster Sound, *Quat. Sci. Rev.*, 91, 184–203,
952 doi:10.1016/j.quascirev.2013.09.025, 2014.
- 953 Polyak, L., Korsun, S., Febo, L. A. and Al., E.: Benthic foraminiferal assemblages from the southern Kara Sea, a
954 river-influenced Arctic marine environment, *J. Foraminifer. Res.*, 32(3), 252–273, doi:10.2113/32.3.252, 2002.
- 955 Pruyssers, P. A., de Lange, G. J. and Middelburg, J. J.: Geochemistry of eastern Mediterranean sediments: Primary
956 sediment composition and diagenetic alterations, *Mar. Geol.*, 100(1–4), 137–154, doi:10.1016/0025-3227(91)90230-
957 2, 1991.
- 958 Ramsey, C. B.: Deposition models for chronological records, *Quat. Sci. Rev.*, 27(1–2), 42–60,
959 doi:10.1016/j.quascirev.2007.01.019, 2008.
- 960 Reimer, P. J., Bard, E., Bayliss, A., Beck, J. W., Blackwell, P. G., Ramsey, C. B., Buck, C. E., Cheng, H., Edwards,
961 R. L., Friedrich, M., Grootes, P. M., Guilderson, T. P., Haflidason, H., Hajdas, I., Hatté, C., Heaton, T. J.,
962 Hoffmann, D. L., Hogg, A. G., Hughen, K. A., Kaiser, K. F., Kromer, B., Manning, S. W., Niu, M., Reimer, R. W.,
963 Richards, D. A., Scott, E. M., Southon, J. R., Staff, R. A., Turney, C. S. M. and van der Plicht, J.: IntCal13 and
964 Marine13 Radiocarbon Age Calibration Curves 0–50,000 Years cal BP, *Radiocarbon*, 55(4), 1869–1887,
965 doi:10.2458/azu_js_rc.55.16947, 2013.
- 966 Renssen, H., Goosse, H. and Fichetef, T.: Contrasting trends in North Atlantic deep-water formation in the Labrador
967 Sea and Nordic Seas during the Holocene, *Geophys. Res. Lett.*, 32(8), L08711, 2005.
- 968 Renssen, H., Seppä, H., Heiri, O., Roche, D. M., Goosse, H. and Fichetef, T.: The spatial and temporal complexity
969 of the holocene thermal maximum, *Nat. Geosci.*, 2(6), 411–414, doi:10.1038/ngeo513, 2009.
- 970 Richter, T. O., Gaast, S. van der, Koster, B., Vaars, A., Gieles, R., Stigter, H. C. de, Haas, H. De and Weering, T. C.
971 E. van: The Avaatech XRF Core Scanner: technical description and applications to NE Atlantic sediments, *Geol.*
972 *Soc. London, Spec. Publ.*, 267(1), 39–50, doi:10.1144/GSL.SP.2006.267.01.03, 2005.



- 973 Rignot, E., Koppes, M. and Velicogna, I.: Rapid submarine melting of the calving faces of West Greenland glaciers,
974 *Nat. Geosci.*, 3(3), 187–191, doi:10.1038/ngeo765, 2010.
- 975 Rothwell, R. G. and Croudace, I. w.: *Micro-XRF Studies of Sediment Cores: A Perspective on Capability and*
976 *Application in the Environmental Sciences*, Springer, Dordrecht., 2015.
- 977 Rykova, T., Straneo, F. and Bower, A. S.: Seasonal and interannual variability of the West Greenland Current
978 System in the Labrador Sea in 1993–2008, *J. Geophys. Res. Ocean.*, 120, 1318–1332, doi:10.1002/2014JC010386,
979 2015.
- 980 Rytter, F., Knudsen, K. L., Seidenkrantz, M.-S. and Eiríksson, J.: Modern distribution of benthic foraminifera on the
981 north Icelandic shelf and slope, *J. Foraminifer. Res.*, 32(3), 217–244, doi:10.2113/32.3.217, 2002.
- 982 Saito, S.: Major and trace element geochemistry of sediments from East Greenland Continental Rise: an implication
983 for sediment provenance and source area weathering, in *Proceedings of the Ocean Drilling Program, 152 Scientific*
984 *Results.*, 1998.
- 985 Schröder-Adams, C. J. and Van Rooyen, D.: Response of Recent Benthic Foraminiferal Assemblages to Contrasting
986 Environments in Baffin Bay and the Northern Labrador Sea , Northwest Atlantic Author (s): CLAUDIA J .
987 SCHRÖDER-ADAMS and DEANNE VAN ROOYEN Source : Arctic , Vol . 64 , No . 3 (SEPTEMBE, Arctic,
988 64(3), 317–341, 2011.
- 989 Scott, D. B., Schell, T., Rochon, A. and Blasco, S.: Benthic foraminifera in the surface sediments of the Beaufort
990 Shelf and slope, Beaufort Sea, Canada: Applications and implications for past sea-ice conditions, *J. Mar. Syst.*,
991 74(3–4), 840–863, doi:10.1016/j.jmarsys.2008.01.008, 2008.
- 992 Seidenkrantz, M.-S.: *Cassidulina teretis* Tappan and *Cassidulina neoteretis* new species (Foraminifera): stratigraphic
993 markers for deep sea and outer shelf areas, *J. Micropalaeontology*, 14, 145–157, 1995.
- 994 Seidenkrantz, M.-S., Ebbesen, H., Aagaard-Sørensen, S., Moros, M., Lloyd, J. M., Olsen, J., Faurschou Knudsen,
995 M. and Kuijpers, A.: Early Holocene large-scale meltwater discharge from Greenland documented by foraminifera
996 and sediment parameters, *Palaeogeogr. Palaeoclimatol. Palaeoecol.*, 391, 71–81, doi:10.1016/j.palaeo.2012.04.006,
997 2013.
- 998 Seidenkrantz, M. S.: Benthic foraminifera as palaeo sea-ice indicators in the subarctic realm - examples from the
999 Labrador Sea-Baffin Bay region, *Quat. Sci. Rev.*, 79, 135–144, doi:10.1016/j.quascirev.2013.03.014, 2013.
- 1000 Seidenkrantz, M. S., Aagaard-Sørensen, S., Sulsbrück, H., Kuijpers, A., Jensen, K. G. and Kunzendorf, H.:
1001 Hydrography and climate of the last 4400 years in a SW Greenland fjord: Implications for Labrador Sea
1002 palaeoceanography, *Holocene*, 17(3), 387–401, doi:10.1177/0959683607075840, 2007.
- 1003 Seidenkrantz, M. S., Roncaglia, L., Fischel, A., Heilmann-Clausen, C., Kuijpers, A. and Moros, M.: Variable North
1004 Atlantic climate seesaw patterns documented by a late Holocene marine record from Disko Bugt, West Greenland,
1005 *Mar. Micropaleontol.*, 68, 66–83, doi:10.1016/j.marmicro.2008.01.006, 2008.
- 1006 Sheldon, C. M., Seidenkrantz, M. S., Pearce, C., Kuijpers, A., Hansen, M. J. and Christensen, E. Z.: Holocene
1007 oceanographic changes in SW Labrador Sea, off Newfoundland, *Holocene*, 26(2), 274–289,
1008 doi:10.1177/0959683615608690, 2016.
- 1009 Sicre, M. A., Weckström, K., Seidenkrantz, M. S., Kuijpers, A., Benetti, M., Masse, G., Ezat, U., Schmidt, S.,
1010 Bouloubassi, I., Olsen, J., Khodri, M. and Mignot, J.: Labrador current variability over the last 2000 years, *Earth*
1011 *Planet. Sci. Lett.*, 400, 26–32, doi:10.1016/j.epsl.2014.05.016, 2014.
- 1012 Ślubowska-Woldengen, M., Rasmussen, T. L., Koç, N., Klitgaard-Kristensen, D., Nilsen, F. and Solheim, A.:
1013 Advection of Atlantic Water to the western and northern Svalbard shelf since 17,500 cal yr BP, *Quat. Sci. Rev.*,
1014 doi:10.1016/j.quascirev.2006.09.009, 2007.
- 1015 Solignac, S., Seidenkrantz, M. S., Jessen, C., Kuijpers, A., Gunvald, A. K. and Olsen, J.: Late-holocene sea-surface
1016 conditions offshore Newfoundland based on dinoflagellate cysts, *Holocene*, 21(4), 539–552,
1017 doi:10.1177/0959683610385720, 2011.
- 1018 Steenfelt, A.: *Geochemical atlas of Greenland – West and South Greenland.*, 2001.
- 1019 Steenfelt, A., Thomassen, B., Lind, M. and Kyed, J.: Karrat 97: reconnaissance mineral exploration in central 761
1020 West Greenland, *Geol. Greenl. Surv. Bull.*, 180, 73–80, 1998.
- 1021 Straneo, F. and Heimbach, P.: North Atlantic warming and the retreat of Greenland’s outlet glaciers, *Nature*,
1022 504(7478), 36–43, doi:10.1038/nature12854, 2013.



- 1023 Straneo, F., Heimbach, P., Sergienko, O., Hamilton, G., Catania, G., Griffies, S., Hallberg, R., Jenkins, A., Joughin,
1024 I., Motyka, R., Pfeffer, W. T., Price, S. F., Rignot, E., Scambos, T., Truffer, M. and Vieli, A.: Challenges to
1025 understanding the dynamic response of Greenland's marine terminating glaciers to oceanic and atmospheric
1026 forcing, *Bull. Am. Meteorol. Soc.*, 94(8), 1131–1144, doi:10.1175/BAMS-D-12-00100.1, 2013.
1027 Tan, F. C., & Strain, P. M.: The distribution of sea ice melt water in the Eastern Canadian Arctic, *J. Geophys. Res.*,
1028 85, 1925–1932, 1980.
1029 Tang, C. C. L., Ross, C. K., Yao, T., Petrie, B., DeTracey, B. M. and Dunlap, E.: The circulation, water masses and
1030 sea-ice of Baffin Bay, *Prog. Oceanogr.*, 63(4), 183–228, doi:10.1016/j.pocean.2004.09.005, 2004.
1031 Tremblay, J.-É., Gratton, Y., Carmack, E. C., Payne, C. D. and Price, N. M.: Impact of the large-scale Arctic
1032 circulation and the North Water Polynya on nutrient inventories in Baffin Bay, *J. Geophys. Res.*, 107(C8), 26-1-26-14, 2002.
1033 Vermassen, F., Andreassen, N., Wangner, D. J., Thibault, N., Seidenkrantz, M. S., Jackson, R., Schmidt, S., Kjær, K.
1034 H. and Andresen, C. S.: A reconstruction of warm-water inflow to Upernavik Isstrøm since 1925 CE and its relation
1035 to glacier retreat, *Clim. Past*, 15(3), 1171–1186, doi:10.5194/cp-15-1171-2019, 2019.
1036 Wang, J., Mysak, L. A. and Grant Ingram, R.: Interannual variability of sea-ice cover in hudson bay, baffin bay and
1037 the Labrador sea, *Atmos. - Ocean*, 32(2), 421–447, doi:10.1080/07055900.1994.9649505, 1994.
1038 Wangner, D. J., Jennings, A. E., Vermassen, F., Dyke, L. M., Hogan, K. A., Schmidt, S., Kjær, K. H., Knudsen, M.
1039 F. and Andresen, C. S.: A 2000-year record of ocean influence on Jakobshavn Isbræ calving activity, based on
1040 marine sediment cores, *Holocene*, 28(11), 1731–1744, doi:10.1177/0959683618788701, 2018.
1041 Weatherall, P., Marks, K. M., Jakobsson, M., Schmitt, T., Tani, S., Arndt, J. E., Rovere, M., Chayes, D., Ferrini, V.
1042 and Wigley, R.: A new digital bathymetric model of the world's oceans, *Earth Sp. Sci.*, 2(8), 331–345,
1043 doi:10.1002/2015EA000107, 2015.
1044 Welford, J. K., Peace, A. L., Geng, M., Dehler, S. A. and Dickie, K.: Crustal structure of Baffin Bay from
1045 constrained three-dimensional gravity inversion and deformable plate tectonic models, *Geophys. J. Int.*, 214(2),
1046 1281–1300, doi:10.1093/GJI/GGY193, 2018.
1047 Wollenburg, J. E. and Kuhnt, W.: The response of benthic foraminifers to carbon flux and primary production in the
1048 Arctic Ocean, *Mar. Micropaleontol.*, 40(3), 189–231, doi:10.1016/S0377-8398(00)00039-6, 2000.
1049 Wollenburg, J. E. and Mackensen, A.: Living benthic foraminifers from the central Arctic Ocean: Faunal
1050 composition, standing stock and diversity, *Mar. Micropaleontol.*, 34, 153–185, doi:10.1016/S0377-8398(98)00007-
1051 3, 1998.
1052 Yang, Q., Dixon, T. H., Myers, P. G., Bonin, J., Chambers, D. and Van Den Broeke, M. R.: Recent increases in
1053 Arctic freshwater flux affects Labrador Sea convection and Atlantic overturning circulation, *Nat. Commun.*, 7,
1054 doi:10.1038/ncomms10525, 2016.
1055 Zreda, M., England, J., Phillips, F., Elmore, D. and Sharma, P.: Unblocking of the Nares Strait by Greenland and
1056 Ellesmere ice-sheet retreat 10,000 years ago, *Nature*, 398, 139–142, doi:10.1038/18197, 1999.
1057